

## HIGHLIGHTED TOPIC | *The Physiology and Pathophysiology of the Hyperbaric and Diving Environments*

# Hyperbaric oxygen stimulates vasculogenic stem cell growth and differentiation in vivo

Tatyana N. Milovanova,<sup>1</sup> Veena M. Bhopale,<sup>1</sup> Elena M. Sorokina,<sup>1</sup> Jonni S. Moore,<sup>2</sup> Thomas K. Hunt,<sup>3</sup> Martin Hauer-Jensen,<sup>4</sup> Omaid C. Velazquez,<sup>5</sup> and Stephen R. Thom<sup>1,6</sup>

<sup>1</sup>Institute for Environmental Medicine, Departments of <sup>2</sup>Pathology and Laboratory Medicine and <sup>6</sup>Emergency Medicine, University of Pennsylvania Medical Center, Philadelphia, Pennsylvania; <sup>3</sup>Department of Surgery, University of California at San Francisco, San Francisco, California; <sup>4</sup>Department of Surgery, University of Arkansas for Medical Sciences, Little Rock, Arkansas; and <sup>5</sup>Department of Surgery, University of Miami, Miami, Florida

Submitted 5 August 2008; accepted in final form 14 November 2008

**Milovanova TN, Bhopale VM, Sorokina EM, Moore JS, Hunt TK, Hauer-Jensen M, Velazquez OC, Thom SR.** Hyperbaric oxygen stimulates vasculogenic stem cell growth and differentiation in vivo. *J Appl Physiol* 106: 711–728, 2009. First published November 20, 2008; doi:10.1152/jappphysiol.91054.2008.—We hypothesized that oxidative stress from hyperbaric oxygen (HBO<sub>2</sub>, 2.8 ATA for 90 min daily) exerts a trophic effect on vasculogenic stem cells. In a mouse model, circulating stem/progenitor cell (SPC) recruitment and differentiation in subcutaneous Matrigel were stimulated by HBO<sub>2</sub> and by a physiological oxidative stressor, lactate. In combination, HBO<sub>2</sub> and lactate had additive effects. Vascular channels lined by CD34<sup>+</sup> SPCs were identified. HBO<sub>2</sub> and lactate accelerated channel development, cell differentiation based on surface marker expression, and cell cycle entry. CD34<sup>+</sup> SPCs exhibited increases in thioredoxin-1 (Trx1), Trx reductase, hypoxia-inducible factors (HIF)-1, -2, and -3, phosphorylated mitogen-activated protein kinases, vascular endothelial growth factor, and stromal cell-derived factor-1. Cell recruitment to Matrigel and protein synthesis responses were abrogated by *N*-acetyl cysteine, dithioerythritol, oxamate, apocynin, U-0126, neutralizing anti-vascular endothelial growth factor, or anti-stromal cell-derived factor-1 antibodies, and small inhibitory RNA to Trx reductase, lactate dehydrogenase, gp91<sup>phox</sup>, HIF-1 or -2, and in mice conditionally null for HIF-1 in myeloid cells. By causing an oxidative stress, HBO<sub>2</sub> activates a physiological redox-active autocrine loop in SPCs that stimulates vasculogenesis. Thioredoxin system activation leads to elevations in HIF-1 and -2, followed by synthesis of HIF-dependent growth factors. HIF-3 has a negative impact on SPCs.

CD34; thioredoxin; hypoxia inducible factor-1; hypoxia inducible factor-2; hypoxia inducible factor-3; mitogen-activated protein kinase; vascular endothelial growth factor; stromal cell-derived factor-1

THE EFFICACY OF HYPERBARIC oxygen (HBO<sub>2</sub>) for healing refractory wounds in diabetic patients and those with radiation injuries has been shown in randomized trials, and its utilization is supported by independent evidence-based reviews (6, 10, 20, 32, 38). Mechanisms of action for HBO<sub>2</sub> are not clear. The goal

of this study was to examine the impact of HBO<sub>2</sub> on vasculogenic stem cells in an in vivo animal model.

In humans, HBO<sub>2</sub> has been shown to stimulate stem/progenitor cell (SPC) mobilization from the bone marrow and improve ex vivo clonal cell growth efficiency (60). In animal models, mobilized SPCs are recruited to wounds and accelerate healing (13, 15). While this response may arise because of the increased numbers of circulating SPCs, cell number alone does not necessarily reflect increased cell recruitment and vasculogenesis at peripheral sites (42). Therefore, we were interested in examining whether HBO<sub>2</sub> may cause changes intrinsic to SPCs that alter cell growth characteristics. We hypothesized that HBO<sub>2</sub> augments SPCs-mediated neovascularization by altering transcription factor expression and growth factor synthesis due to an oxidative stress response.

Reactive oxygen species (ROS) are a trophic stimulus to SPCs (42). For example, under normal physiological conditions, increasing the tissue lactate concentration will increase cellular NADH through the action of lactate dehydrogenase (LDH), and this secondarily increases intracellular ROS production by stimulating NAD(P)H oxidase (Nox) enzymes (18, 35, 42). Lactate can also enhance free radical formation via Fenton-like reactions (2, 18). Lactate metabolism by SPCs accelerates progressive SPCs recruitment to target sites remote from the bone marrow. This occurs because of a complex set of responses initiated by thioredoxin (Trx)-1 (Trx1) synthesis in response to oxidative stress, which elevates hypoxia inducible factor-1 (HIF-1) and HIF-1-dependent growth factors (42). Local tissue lactate concentration is elevated in wounds and reaches to ~6–15 mM, in contrast to a concentration of 1.8–2 mM under nonwounded conditions (14, 65).

Trx are ubiquitous disulfide oxidoreductase proteins that work in conjunction with the glutathione system to maintain the cytoplasm in a reduced state. The Trx system includes the Trx1 cytosolic and Trx2 mitochondrial thiol proteins, Trx reductase (TrxR) and NADPH. Oxidative stress increases Trx1 synthesis and its translocation to the nucleus, where Trx1 will act as a growth factor and transcription factor regulator (4, 12,

Address for reprint requests and other correspondence: S. R. Thom, Institute for Environmental Medicine, Univ. of Pennsylvania, 1 John Morgan Bldg., 3620 Hamilton Walk, Philadelphia, PA 19104-6068 (e-mail: sthom@mail.med.upenn.edu).

The costs of publication of this article were defrayed in part by the payment of page charges. The article must therefore be hereby marked “advertisement” in accordance with 18 U.S.C. Section 1734 solely to indicate this fact.

21, 44, 52). There are redundant systems for maintaining Trx1 in a reduced state, which is fundamental to regulating its functions. Knocking down TrxR either by enzyme inhibitors or small inhibitory RNA (siRNA) will significantly deplete the cellular concentration of reduced Trx1 under conditions of oxidative stress (67).

Trx1 promotes the expression and activity of HIF-1 (12, 26, 68). HIF transcription factors are heterodimers of HIF- $\alpha$  and a constitutively expressed HIF- $\beta$  (also called the aryl hydrocarbon receptor nuclear translocator subunit). There are three HIF- $\alpha$  proteins. HIF-1 and -2 coordinate many cell responses involved with neovascularization by regulating gene transcription, and, while there is overlap in their activities, there are also a number of genes preferentially regulated by either HIF-1 or -2 (66). The biological function of HIF-3 is unclear, and at least one splice variant negatively modulates HIF-1 and -2, although its expression is tissue restricted (37, 41).

The expression and activation of HIF- $\alpha$  subunits are tightly regulated. When cells are replete with O<sub>2</sub>, HIF- $\alpha$  degradation by the ubiquitin-proteasome pathway can occur via the action of ferrous iron and O<sub>2</sub>-dependent prolyl hydroxylase enzymes (53, 55). There are also many pathways for augmenting HIF- $\alpha$  expression and activity under normoxic conditions. Translational regulation of HIF-1 by a variety of growth factors, tumor suppressors, and cytokines involves ROS production (8, 16, 36, 45, 49). Trx1 will increase HIF-1 protein expression and activity under both normoxic and hypoxic conditions, and oxidation of cellular ascorbate and ferrous iron diminishes HIF-1 $\alpha$  degradation by impeding prolyl hydroxylase enzymes (31, 45, 68). Factors and conditions controlling HIF-2 and -3 are not as well defined.

HIF-1 and -2 coordinate cell responses important for neovascularization, including synthesis of vascular endothelial growth factor (VEGF) and stromal cell-derived factor 1 (SDF-1) (51). These growth factors, and others, are synthesized by local endothelial cells, perivascular myofibroblasts, keratinocytes, macrophages, bone marrow-derived hemangiocytes, and endothelial progenitor cells recruited to peripheral sites (17, 25, 39, 54, 56). Growth factors influence the efficiency of new blood vessel growth by angiogenesis involving local endothelial cells, and they stimulate the recruitment and differentiation of circulating SPCs to form vessels by de novo vasculogenesis (15, 22, 50, 57, 62, 70).

We hypothesized that ROS from HBO<sub>2</sub> exposure augment SPC growth and differentiation. The focus of this investigation was to evaluate whether oxidative stress occurs due to HBO<sub>2</sub> and then assess SPC-mediated vasculogenesis. In the mouse model, SPCs are among the earliest cells to arrive at subcutaneous Matrigel "targets" (42). Results show that HBO<sub>2</sub> as well as lactate markedly augment SPC recruitment and differentiation, and there are roles for all three HIF isoforms. HBO<sub>2</sub> accelerates neovascularization by increasing the number of SPCs in blood (and thus the number of cells available to home to target tissues), and by increasing levels of cellular transcription factors. HBO<sub>2</sub> stimulates SPC growth and differentiation by engaging a physiological autocrine activation loop responsive to oxidative stress.

## EXPERIMENTAL PROCEDURES

**Animal procedures.** Wild-type mice (*Mus musculus*) were purchased (Jackson Laboratories, Bar Harbor, ME), fed a standard rodent diet and water ad libitum, and housed in the animal facility of the University of Pennsylvania. In some studies, we used mice with conditional HIF-1 null myeloid cells developed by Dr. Randall S. Johnson at the University of California, San Diego. In these mice, Cre recombinase cDNA was inserted into the endogenous myeloid lysozyme locus, along with loxP flanking the HIF-1 locus. All aspects of this investigation were reviewed and approved by the Institutional Animal Care and Use Committee.

The standard protocol and all procedures are described in detail in a previous publication (42). In brief, the approach was to place two subcutaneous Matrigel plugs under sterile conditions, one on either side of the thoracic vertebrae of an anesthetized mouse. One of the Matrigel plugs was supplemented with DL-lactide (85 mol%, 32 mg/ml Matrigel). This polymer is slowly hydrolyzed so that, when applied to wounds, it will sustain the lactate monomer concentration within a range of ~6–15 mM (63). In our studies, slow degradation of the lactate polymer resulted in a lactate concentration in Matrigel of  $16.2 \pm 0.4$  mM (means  $\pm$  SE;  $n = 3$ ) at 18 h after implantation vs.  $3.5 \pm 0.7$  mM ( $n = 3$ ,  $P < 0.05$ ) in unsupplemented Matrigel. Levels remained stable over the course of the experiment, and, at 10 days, values were  $15.8 \pm 0.3$  mM ( $n = 3$ ) for lactide-supplemented Matrigel and  $3.8 \pm 0.5$  mM ( $n = 3$ ) for unsupplemented Matrigel. Lactate concentration in digested Matrigel was measured by Enzy-Chrom Lactate Assay Kit (Bioassay Systems, Hayward, CA). Lactate, a weak base, had an effect on Matrigel pH. Immediately after lactide was dissolved in Matrigel, the pH was assessed by touching a sample to a piece of Hydriion pH paper. Unsupplemented Matrigel had a pH of  $7.90 \pm 0.03$  (mean  $\pm$  SE,  $n = 7$ ), and Matrigel + lactide had a pH of  $8.4 \pm 0.07$  ( $n = 7$ ,  $P < 0.05$ ). The pH of samples removed from mice 18 h after implantation was  $7.46 \pm 0.02$  ( $n = 7$ ,  $P < 0.05$  vs. the value before implantation) in unsupplemented Matrigel, and in Matrigel + lactide it was  $7.63 \pm 0.04$  ( $n = 7$ ,  $P < 0.05$  vs. value before implantation and vs. value in unsupplemented samples removed at 18 h).

Chemicals were purchased from Sigma except where noted otherwise. For some studies, Matrigel was supplemented with 15 mM oxamate, 10  $\mu$ M mitomycin C, 0.1 mM apocynin, 1  $\mu$ M dithioerythritol (DTE), 5  $\mu$ M *N*-acetyl cysteine (NAC), 10 mM 3-amino-1,2,4-triazole (ATZ), 14  $\mu$ M 1,4-diamino-2,3-dicyano-1,4,6 [2-aminophenylthio] butadiene (U-0126, Calbiochem, San Diego, CA), and 10  $\mu$ g anti-VEGF or anti-SDF1 (from BD Bioscience, San Diego, CA). siRNA sequences were purchased from commercial vendors, and 37.5 ng were placed in individual 1-ml Matrigel samples before injection, as described previously (42). The siRNA to HIF-1, HIF-2, or HIF-3, TrxR, gp91<sup>phox</sup> Nox subunit, or nonsilencing control siRNA conjugated to AlexaFluor 488 were purchased from Qiagen (Germantown, MD), and siRNA specific to mouse LDH was purchased from Santa Cruz Biotechnology (Santa Cruz, CA).

Where identified, mice were exposed to HBO<sub>2</sub> at 2.8 ATA for 90 min following published procedures (60). The first exposure occurred within 2 h of Matrigel implantation, once mice recovered from anesthesia. The second exposure occurred 12 h later, so that mice killed 18 h postimplantation received two separate HBO<sub>2</sub> exposures. Other mice received HBO<sub>2</sub> on a daily basis for a total of 5 or 10 consecutive days. Sham and pressure-only (no hyperoxia) controls were not performed in these trials, as previous work has established that these manipulations do not modify SPC mobilization and growth characteristics (60).

At selected times, mice were reanesthetized, and blood was obtained into heparinized syringes by cardiac puncture. Matrigel plugs were harvested, sharply cut with a blade, and, where indicated, approximately one-third was placed in Metho-Cult colony assay medium (StemCell Technologies, Vancouver, BC) for incubation at 37°C, air with 5% CO<sub>2</sub>, in a fully humidified atmosphere. In other

studies, a small slice of the Matrigel was placed on a glass slide for staining with 10  $\mu\text{M}$  2',7'-dichlorofluorescein ( $\text{H}_2\text{DCF}$ , Kodak, Rochester, NY) diacetate or fluorochrome-conjugated antibodies for microscopic examination, and in all trials the remaining Matrigel plug was weighed in plastic dishes and then digested by incubation with 1 ml Dispase for 90 min at 37°C.

DCF fluorescence measurements were carried out on Matrigel plugs following published techniques (42). Comparison among the samples was performed by first measuring cell fluorescence and then moving the microscope objective to add several drops of 24 mM KCl to cause cell depolarization, and remeasuring fluorescence at the same site. Expressing sample fluorescence as a ratio using the signal obtained after cell depolarization provided a way to control for different numbers of cells in the various samples. There were several special aspects to the method used in this study pertaining to measurements performed after  $\text{HBO}_2$ . The high fluorescence signals obtained required use of different sensitivity settings than were used in a prior publication (42). Another special aspect to the DCF studies was that mice were exposed to hyperoxia and promptly anesthetized for Matrigel harvesting so that microscopic analysis was done within a span of  $\sim 15$  min. If harvesting and analysis were delayed by over 30 min, no elevations in DCF fluorescence were discernible over the air-exposed control mice, which we interpret as occurring because elevations in Matrigel  $\text{O}_2$  content had dissipated.

Bone marrow cells were also obtained from both femurs. The ends of each bone were clipped, and the marrow cavities flushed with 2 ml phosphate-buffered saline. Leukocytes were isolated from blood, Matrigel digested with Dispase, and bone marrow for cell counts, flow cytometry analysis, and Western blotting of cell lysates. In addition, the cells from digested Matrigel were frozen and subjected to Western blotting at later times. In brief,  $5 \times 10^6$  cells from each location (Matrigel, blood or bone marrow) were lysed and adjusted to 25 mg protein/ml, 5  $\mu\text{g}$  protein were placed in each lane, and Western blots were performed following published methods (60). Antibodies used for Western blotting were against HIF-1, HIF-2, or HIF-3 (R&D Systems, Minneapolis, MN), catalase,  $\beta$ -actin, VEGF, SDF-1, TrxR, Trx1 (Cell Signaling Technology, Danvers, MA), and the phosphor-specific and total MAPKs ERK1/2, JNK (Santa Cruz), and p38 (BD Pharmingen).

**Flow cytometry.** Flow cytometry was performed with a four-color, dual-laser analog FACSCalibur (Becton Dickinson, San Jose, CA) using CellQuest acquisition software, or 18-color LSRII (BD Bioscience, San Diego, CA) using FACSDiva digital acquisition electronics and software (BD Bioscience) by standard protocol (42). Cells were gated based on forward and side laser light scatter and nucleated cells segregated from debris by DRAQ5 DNA staining. To identify SPCs, we utilized specific anti-mouse fluorochrome-conjugated antibodies and measured cell surface fluorescence, as described in detail in a previous report (42). Antibodies used in this study were as follows: CD34-fluorescein isothiocyanate (FITC), CD34-phycoerythrin (eBioscience, San Diego, CA, and BD Pharmingen), Sca-1(FITC) (BD Pharmingen), CXCR4-allophycocyanin (APC) (R&D, Minneapolis, MN), VEGFR2(Flk-1)-APC, von Willebrand factor (vWF)-FITC, CD133-APC, and TER119-FITC (eBioscience). Cell cycle analysis and the fraction of dead cells were assessed based on propidium iodide staining of  $1 \times 10^6$  leukocytes using ModFit LT Cell Cycle Analysis Software (Verity Software House) (42).

**Intracellular protein staining for flow cytometry.** Isolated leukocytes ( $5 \times 10^5$ ) were pelleted, fixed with 4% paraformaldehyde, washed, and stained as described (42). Cells were permeabilized and stained for intracellular Trx1, TrxR, gp91<sup>phox</sup>, HIF-1, HIF-2, or HIF-3, as well as  $\beta$ -actin, and surface stained for the presence of CD34 and CD45. Cells were analyzed by flow cytometry, and data were analyzed using CellQuest (Becton Dickinson) or FlowJo (TreeStar) software.

**Confocal microscopy.** Confocal microscopy (Radiance 2000, BioRad, Hercules, CA) was used to image vascular channels and cells

recruited into Matrigel. Matrigel implants were thin-sliced, and cells were labeled with specific anti-mouse CD34-FITC, TER119-FITC, vWF-FITC, or CD31-FITC, in 1:100 dilutions for 60 min on ice, and then placed on a glass slide for observation at  $\times 600$  and 5 times  $\times 600$  magnification. The presence of functional vascular channels in the Matrigel was documented by injecting mice with carboxylate-modified polystyrene beads (FluoSpheres, Invitrogen, 0.04  $\mu\text{m}$ ) conjugated to Nile red or FITC-conjugated dextran (40,000 mol wt, Invitrogen) following published procedures (42).

**Determination of in vivo  $\text{H}_2\text{O}_2$  production.** Production of  $\text{H}_2\text{O}_2$  by cells in Matrigel was evaluated by measuring ATZ-dependent inhibition of catalase. For these trials, Matrigel was supplemented with the  $\text{H}_2\text{O}_2$ -dependent catalase inhibitor ATZ before injections, and residual catalase activity was measured in SPCs lysates obtained 18 h later following published methods (61). In brief, specific catalase activity in lysates was expressed as units of activity/gram cell protein [1 unit = decomposition of 1  $\mu\text{mol}$   $\text{H}_2\text{O}_2$ /min at 25°C (pH 7.0) using the  $\text{H}_2\text{O}_2$   $\epsilon_m = 43.6 \text{ M}^{-1}\text{cm}^{-1}$ , where  $\epsilon_m$  is the extinction coefficient]. Differences in  $\text{H}_2\text{O}_2$  production by cells in vivo were reflected by the difference in catalase activity among lysates from Matrigel without vs. Matrigel with ATZ added. Catalase content in cell lysates was also assessed by Western blots and normalized to the presence of  $\beta$ -actin in the same samples.

**Measurements of reduced and oxidized glutathione.** Using SPCs lysates obtained 18 h or 5 or 10 days after Matrigel implantation, acid-soluble oxidized glutathione (GSSG) and total glutathione (GSH + GSSG) were measured spectrophotometrically at 412 nm by the GSSG reductase recycling assay with 5,5'-dithiobis (2-nitrobenzoic acid) (1).

**Statistical analysis.** Results are expressed as the mean  $\pm$  SE for three or more independent experiments. To compare data, we used a one-way ANOVA using SigmaStat (Jandel Scientific, San Jose, CA) and Newman-Keuls post hoc test, or Student's *t*-tests, where appropriate. The level of statistical significance was defined as  $P < 0.05$ .

## RESULTS

**Vascular channels in matrigel.** Vascularized channels can be found in Matrigel 18 h after implantation in mice (42). Our goal in this investigation was to evaluate channel formation in Matrigel from  $\text{HBO}_2$ -exposed vs. control, air-breathing mice. Channels were visualized following intracardiac infusion of fluorescein-conjugated Dextran or Nile red beads before harvesting Matrigel (Fig. 1A). Many CD34<sup>+</sup> cells also expressed the endothelial progenitor cell marker, CD31, and the mitotic marker, Ki67.

Channels lined by CD34<sup>+</sup> cells appeared to be more numerous and with a greater anastomotic network in  $\text{HBO}_2$  exposed vs. control mice. To quantify perceived differences, Nile red fluorescence was measured to evaluate perfusion, and Matrigel sections were stained for the SPC marker CD34, as well as for CD45<sup>+</sup> leukocytes. Significantly more fluorescence due to the presence of beads, as well as cells, was detected in samples from  $\text{HBO}_2$  mice, and still more in samples containing the lactate polymer (Fig. 1B). As expected, there was colocalization between channels and both types of cells, but CD45<sup>+</sup> cells were few and exhibited relatively dim fluorescence. In contrast, CD34<sup>+</sup> cell and bead fluorescence were nearly 100-fold brighter and closely aligned, as shown in the plot in Fig. 1B.

**Matrigel cell counts.** Cells present in Matrigel were evaluated by flow cytometry at 18 h, 5 days, or 10 days after implantation (Fig. 2). Most were positive for CD34, and infiltration by other cell types was low. Non-SPC infiltration at 18 h postimplantation was estimated by counting CD45<sup>+</sup>/CD34<sup>-</sup> leukocytes, and these cells accounted for no more than

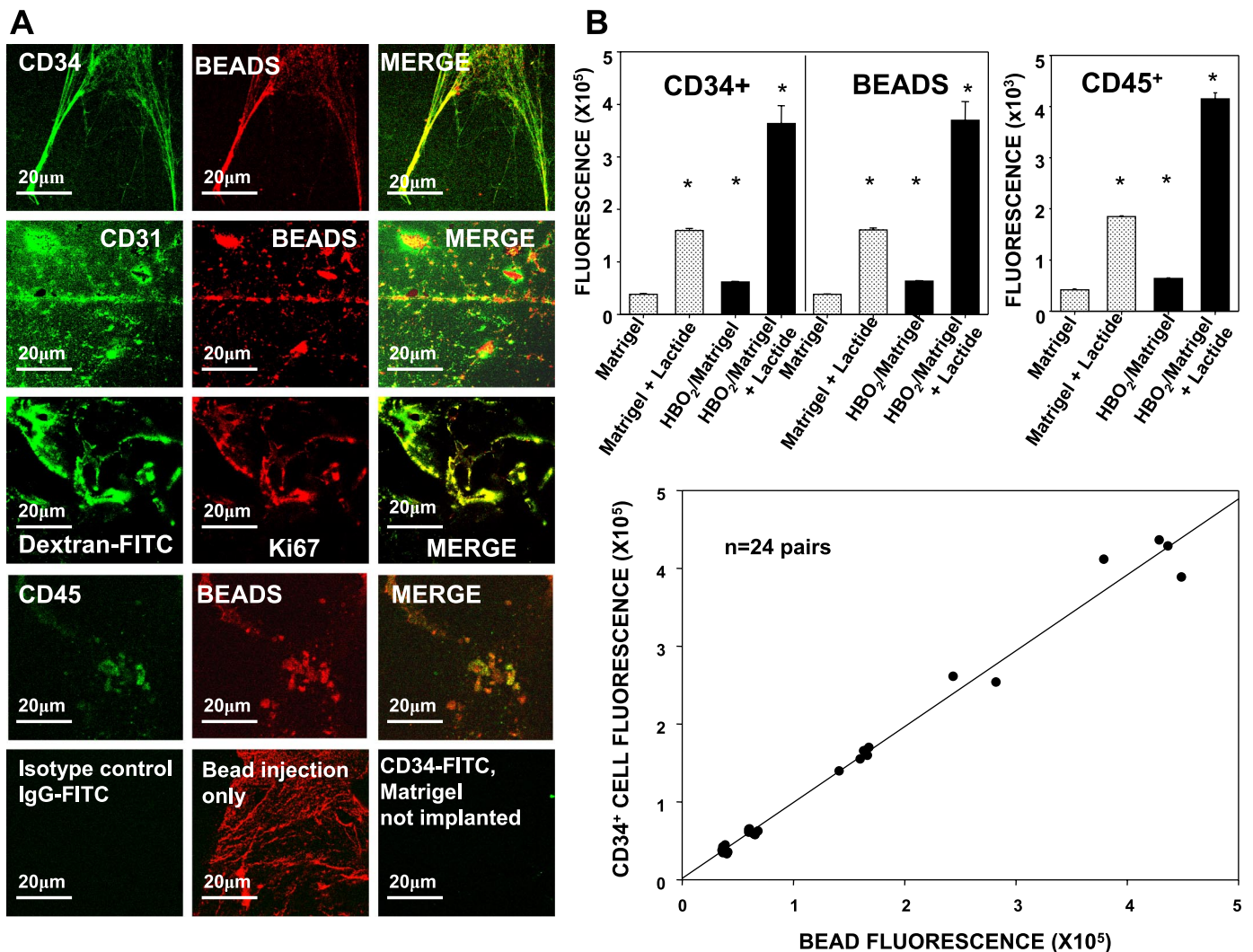


Fig. 1. A: surface marker expression and vascular channels identified by dextran and Nile red beads in Matrigel harvested 18 h postimplantation. The first three rows show images of SPCs from different hyperbaric oxygen (HBO<sub>2</sub>)-exposed mice. The fourth row shows dim fluorescence of CD45<sup>+</sup> leukocytes in Matrigel harvested at 18 h and poor colocalization with Nile red beads. The *bottom* row shows results from representative control studies where no antibody or only nonspecific fluorochrome-conjugated antibodies were used, or Matrigel that was not implanted into mice was staining with CD34-FITC conjugated antibody. B, *top*: fluorescence intensity (arbitrary units) of Matrigel samples. Evaluations were performed on separate samples from 6–8 different mice. Values are means  $\pm$  SE for each determination. \*Significantly different from fluorescence intensity in unsupplemented Matrigel from air-exposed, control mice. The fluorescence intensities in Matrigel + lactide samples were all significantly greater than those for unsupplemented Matrigel, and intensity of matched samples (+/- lactide) from HBO<sub>2</sub>-exposed mice was significantly greater than for air-exposed, control mice. B, *bottom*: correlation between CD34<sup>+</sup> cell fluorescence and Nile red bead fluorescence using data from 24 separate analyses.

10% of the total. In air-exposed, control mice, unsupplemented Matrigel had  $1.5 \pm 0.03 \times 10^5$  CD45<sup>+</sup>/CD34<sup>-</sup> leukocytes (mean  $\pm$  SE,  $n = 10$ ), and in Matrigel + lactide there were  $5.6 \pm 0.19 \times 10^5$  CD45<sup>+</sup>/CD34<sup>-</sup> cells ( $n = 10$ ,  $P < 0.05$  vs. unsupplemented Matrigel). In HBO<sub>2</sub>-exposed mice, the number of CD45<sup>+</sup>/CD34<sup>-</sup> leukocytes in unsupplemented Matrigel was significantly lower than in the air-exposed controls,  $0.87 \pm 0.05 \times 10^5$  ( $n = 10$ ,  $P < 0.05$ ). Similarly, the CD45<sup>+</sup>/CD34<sup>-</sup> leukocyte count in Matrigel + lactide from HBO<sub>2</sub>-exposed mice was less than in air-exposed controls,  $2.6 \pm 0.06 \times 10^5$  ( $n = 10$ ,  $P < 0.05$ ). Cell counts increased at 5 days postimplantation. Among the cell counts for plugs harvested at 10 days, the only samples showing significantly more cells than the 5-day samples were from Matrigel without lactide in HBO<sub>2</sub>-exposed mice.

**SPC recruitment vs. proliferation in Matrigel.** To evaluate recruitment of cells to Matrigel from the circulation vs. local proliferation, mitomycin C was added to Matrigel as a cytostatic agent before injection. The number of CD34<sup>+</sup> cells was essentially the same between standard Matrigel samples and those containing mitomycin C (Table 1), indicative of SPC recruitment as the primary basis for the cell numbers at 18 h postimplantation. The cytostatic impact on mitomycin C in both the control and HBO<sub>2</sub>-exposed mice was apparent based on cell apoptosis assessed by annexin V expression.

**SPC characterization.** Differences in Matrigel cell counts between air-exposed control mice and those exposed to HBO<sub>2</sub> were clearly established at 18 h postinjection, so we wanted to evaluate the CD34<sup>+</sup> population at this time. Surface markers in addition to CD34 were evaluated to more precisely assess the

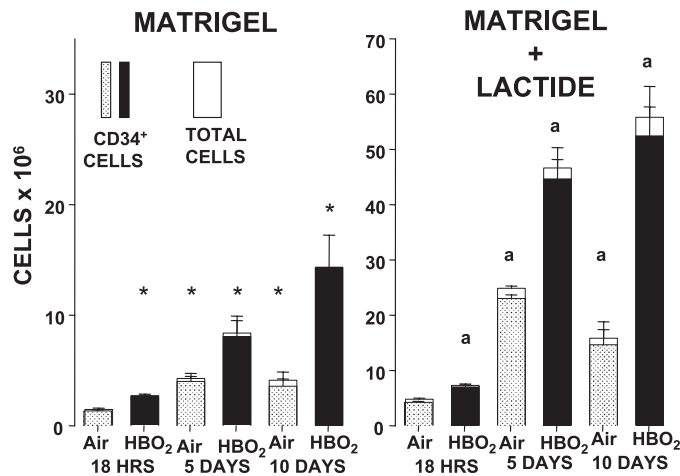


Fig. 2. CD34<sup>+</sup> and total cell counts in Matrigel plugs. Plugs were digested with Dispase, stained with fluorochrome-tagged antibodies, and suspended in phosphate-buffered saline. Total number in each sample was calculated based on the volume of cell suspension and the rate that fluid was taken up in the flow cytometer. At each time point in both Matrigel and Matrigel + lactide figures, the cell counts in HBO<sub>2</sub>-exposed mice were significantly greater than counts in air-exposed, control mice. Also, all cell counts in Matrigel + lactide samples (right) are significantly greater than those in unsupplemented Matrigel (left) harvested at the same time. \*Significantly different than cell number in unsupplemented Matrigel harvested at 18 h on left for unsupplemented Matrigel. <sup>a</sup>Significantly different than cell number in 18 h-Matrigel + lactide sample in air-exposed, control mice. Cell counts in unsupplemented Matrigel harvested from HBO<sub>2</sub>-exposed mice at 5 vs. 10 days postimplantation are also significantly different. Values are means ± SE; n = 10 for 18 h samples, n = 5 for other groups.

lineage of cells. Table 2 shows coexpression of markers on CD34<sup>+</sup> cells from bone marrow, blood, and Matrigel +/- lactide 18 h postimplantation. In control mice, the fraction of cells expressing putative SPC markers, including dim surface expression of CD45 (CD45<sup>-</sup>), Sca-1, CD133, and CXCR4, were lower in blood than in bone marrow, as expected (5). There were no significant differences in CD34<sup>+</sup> cell surface expression of these markers between bone marrow and blood for HBO<sub>2</sub>-exposed mice.

CD31 and VEGFR2, which are thought to be expressed by endothelial cell progenitors, were found in a small population of bone marrow CD34<sup>+</sup> cells, and in 46–97% of CD34<sup>+</sup> cells in the blood. Approximately twice as many CD34<sup>+</sup> cells in the blood of HBO<sub>2</sub>-exposed mice expressed CD31 vs. control mice. Expression of vWF was found in approximately one-third of CD34<sup>+</sup> cells in bone marrow, but a very small fraction of CD34<sup>+</sup> cells in the blood. The population coexpressing vWF in the HBO<sub>2</sub>-exposed mice vs. controls was significantly

larger in all samples (bone marrow, blood, and Matrigel +/- lactide). We also evaluated DRAQ5 (nucleated) cell expression of TER119, a surface marker for cells following an erythroid lineage (28), because erythrocytes are found within vascular channels lined with CD34<sup>+</sup> cells (42). As shown in Table 2, few CD34<sup>+</sup> cells in blood expressed TER119, but the population coexpressing TER119 was significantly higher in all samples from HBO<sub>2</sub>-exposed vs. control mice.

**Cell proliferation in Matrigel.** To explore local proliferation of cells in Matrigel, plugs were harvested 18 h after implantation and incubated ex vivo for 7 days (Table 3). Whereas air-exposed, control cells and those obtained from HBO<sub>2</sub>-exposed mice demonstrated increased cell numbers, there were significantly greater numbers in Matrigel from HBO<sub>2</sub>-exposed mice. Lactide and HBO<sub>2</sub> also influenced differentiation based on surface marker expression. Significantly more CD34<sup>+</sup> cells expressed CD45 after the 7-day incubation vs. 18 h in all samples (compare values in Tables 2 and 3), but there was a much greater elevation in lactide-containing Matrigel. Cell recruitment at 18 h (compare with Table 1), and ex vivo proliferation over 7 days was suppressed if Matrigel contained oxamate, a competitive LDH inhibitor, or antibodies against VEGF or SDF-1. These agents also reduced elevations in fraction of cells expressing CD45 or TER119.

**Effects of antioxidants on SPC recruitment.** Oxidative stress mediated by lactate metabolism is a trophic stimulus for SPCs (42), so we examine the impact of CD34<sup>+</sup> cell recruitment to Matrigel that included antioxidants (Fig. 3). Some of the data from the air-exposed, control mice were presented in another publication, and are shown here to ease comparisons (42). Experiments with the control and HBO<sub>2</sub>-exposed mice were performed concurrently. The number of SPCs was significantly reduced in Matrigel that included siRNA to LDH or the gp91<sup>phox</sup> Nox subunit, apocynin (a Nox oxidase inhibitor), or the antioxidants NAC or DTE. We also evaluated the impact of siRNA to TrxR, because the Trx system responds to oxidative stress by altering transcription and growth factor synthesis (44, 52). All of the agents caused significant inhibition of SPC recruitment to Matrigel in mice, whether they were exposed to HBO<sub>2</sub> or not. In HBO<sub>2</sub>-exposed mice, agents reduced SPC recruitment to unsupplemented Matrigel to levels comparable to numbers found in unsupplemented Matrigel of control, air-exposed mice. Augmented SPC recruitment was still apparent, however, in lactide-containing Matrigel vs. that found in unsupplemented Matrigel (note difference in ordinate scales between sample types). In these trials, reduced content of a specified protein due to siRNA addition was evaluated in permeabilized cells by flow cytometry. Fluorescence with

Table 1. CD34<sup>+</sup> cells in Matrigel

	n	Air Exposed (Control)		HBO <sub>2</sub>	
		Matrigel	Matrigel + lactide	Matrigel	Matrigel + lactide
No addition, ×10 <sup>6</sup>	14	1.3±0.1	4.2±0.2*	2.6±0.1†	7.1±0.3*†
Annexin V positive, %		5.9±1.8	4.6±0.8	3.1±1.8	1.8±1.0
+Mitomycin C, ×10 <sup>6</sup>	3	1.7±0.1	4.8±0.1*	2.9±0.1†	7.8±0.1*†
Annexin V positive, %		62.3±2.3	66.0±3.0	54.6±1.3	62.5±1.3

Values are means ± SE; n, no. of animals. CD34<sup>+</sup> cells were counted for each sample. HBO<sub>2</sub>, hyperbaric oxygen. \*Significantly different from unsupplemented Matrigel, P < 0.05. †Significantly different from air-exposed, control, P < 0.05. Cell counts in samples containing mitomycin C were not different from those without the agent shown in the top row. There were significantly more annexin V positive cells in all samples supplemented with mitomycin C.

Table 2. Surface markers expression on CD34<sup>+</sup> cells measured by four-color flow cytometry

CD34 <sup>+</sup> /Surface Marker/DRAQ5 <sup>+</sup>	Bone Marrow		Blood		Matrigel		Matrigel/Lactide	
	Air	HBO <sub>2</sub>	Air	HBO <sub>2</sub>	Air	HBO <sub>2</sub>	Air	HBO <sub>2</sub>
CD45 <sup>-</sup>	94±3	97±2	80±4*	96±4	95±2	97±2	88±2*	96±3
Sca-1 <sup>+</sup>	95±2	98±2	79±3*	94±5	96±1	98±2	92±3	96±4
CD133 <sup>+</sup>	90±4	93±4	66±2*	88±3	95±3	97±2	82±3*	97±6
CXCR4 <sup>+</sup>	78±2	82±8	56±5*	86±4	90±5	94±3	80±5*	89±2
CD31 <sup>+</sup>	4±2	6±3	46±4*	76±6	82±4*	90±4	86±3*	92±7
VEGFR <sup>+</sup>	6±2	8±4	97±2	96±4	92±4	97±2	90±4	96±4
vWF <sup>+</sup>	26±3*	46±4	4±1*	8±2	6±2*	26±5	66±4*	93±3
TER119 <sup>+</sup>	42±3*	67±3	3±1*	7±2	42±4*	56±4	42±6*	62±8

Values are means ± SE fraction (%) of cells; *n* = 5 animals. vWF, von Willebrand factor. A minimum of 50,000 CD34<sup>+</sup> cells were counted for each sample. \*Significantly different from HBO<sub>2</sub> value in the same group (bone marrow, blood, Matrigel, or Matrigel + lactide).

APC-conjugated antibody to LDH, gp91<sup>phox</sup>, or TrxR in the CD34<sup>+</sup> cells was at the background level, the same magnitude as occurred with nonspecific APC-conjugated antibody. An example of this analysis conducted in cells from Matrigel-containing siRNA to gp91<sup>phox</sup> is shown in Fig. 4.

**Enhanced oxidant production in matrigel-sequestered cells by HBO<sub>2</sub>.** ROS production by SPCs was evaluated using two methods. First, Matrigel harvested 18 h after implantation was stained with H<sub>2</sub>DCF, and its conversion to fluorescent DCF was measured. Results in Fig. 5A are expressed as a ratio compared with the fluorescence achieved by adding 24 mM KCl, which causes cell depolarization. HBO<sub>2</sub> caused a significant elevation in ROS production compared with samples from air-exposed, control mice. Consistent with prior studies (42), including the lactate polymer, increased ROS production. The values shown in the four sample types in Fig. 5A are all significantly different from each other, such that ROS production follows the order HBO<sub>2</sub> exposed, Matrigel + lactide > HBO<sub>2</sub> exposed, Matrigel > air-exposed, Matrigel + lactide > air-exposed, Matrigel.

Intracellular H<sub>2</sub>O<sub>2</sub> production by cells sequestered in the Matrigel was assessed as a second method to verify that HBO<sub>2</sub> caused elevated ROS production in SPCs (Fig. 5B). H<sub>2</sub>O<sub>2</sub> production was evaluated by measuring the disappearance of catalase activity in cell lysates obtained from Matrigel samples containing the irreversible inhibitor, ATZ, and comparing

results with standard Matrigel samples. Decreases in catalase activity indicate an increase in the formation of ATZ-H<sub>2</sub>O<sub>2</sub>-catalase triplex. At nonrate-limiting ATZ concentrations, formation of the triplex is pseudo-first order with respect to time and H<sub>2</sub>O<sub>2</sub> concentration (69). Samples from mice exposed to HBO<sub>2</sub> demonstrated significantly greater differences between ATZ supplemented vs. unsupplemented samples, indicative of augmented H<sub>2</sub>O<sub>2</sub> production. Lactate-supplemented samples also exhibited elevations in H<sub>2</sub>O<sub>2</sub> production vs. unsupplemented Matrigel. Based on the differences in catalase activity of samples without and with ATZ, relative H<sub>2</sub>O<sub>2</sub> production followed the order HBO<sub>2</sub> exposed, Matrigel + lactide > HBO<sub>2</sub> exposed, Matrigel = air-exposed, Matrigel + lactide > air-exposed, Matrigel. We also found significantly higher expression of catalase in HBO<sub>2</sub>-exposed cells, as well as those from lactide-supplemented samples, indicative of an oxidative stress response (Fig. 5B).

**Glutathione measurements.** The content of GSSG and GSH was measured in cell lysates from Matrigel harvested 18 h or 5 or 10 days after implantation (Fig. 6). Consistent with findings that ROS are generated by lactate and HBO<sub>2</sub>, each of these stimuli causes significant increases in total glutathione (GSH + GSSG). There was also a general pattern of increases in total glutathione per milligram protein content over time (18 h to 10 days) within each group. Mean values of GSH and GSSG, as well as statistically significant differences across

Table 3. CD34<sup>+</sup> cell count in Matrigel harvested 18 h postimplantation and incubated ex vivo for 7 days and proportion coexpressing CD45 or TER119

Day 7	<i>n</i>	Air		HBO <sub>2</sub>	
		Matrigel	Matrigel + lactide	Matrigel	Matrigel + lactide
Controls, ×10 <sup>6</sup>	5	31.5±6.1	88.3±20.3*	89.6±33.2*	126.4±30.5†
CD45, %		44.1±12.1	81.3±6.2*	43.3±4.9	89.4±4.6†
TER119, %		39.5±4.5	48.6±2.8	47.8±8.1	84.5±4.9†
+Oxamate, ×10 <sup>6</sup>	3	16.2±2.8‡	44.3±4.1*‡	46.4±3.6*‡	69.0±5.7*‡
CD45, %		18.9±3.1‡	36.2±4.4‡	20.6±2.7‡	45.8±4.6‡
TER119, %		22.4±6.1‡	34.3±1.6‡	25.2±2.8‡	39.6±5.2‡
+Anti-VEGF, ×10 <sup>6</sup>	3	20.2±3.4‡	48.7±7.4*‡	52.8±7.6*‡	74.8±2.2*‡
CD45, %		23.4±2.2‡	39.8±6.4‡	28.3±3.1‡	49.9±6.8‡
TER119, %		26.7±2.8‡	30.1±3.5‡	28.7±3.0‡	32.1±3.4‡
+Anti-SDF-1, ×10 <sup>6</sup>	3	14.7±1.9‡	30.6±5.4*‡	36.1±4.3*‡	55.5±3.8*‡
CD45, %		12.8±1.5‡	28.6±2.8‡	20.3±2.4‡	30.7±5.1‡
TER119, %		19.7±4.5‡	23.5±2.4‡	26.9±2.8‡	19.4±4.0‡

Values are means ± SE; *n*, no. of animals. SDF-1, stromal cell-derived factor 1. \*Significantly greater than cell number in unsupplemented Matrigel samples from air-exposed, control mice, *P* < 0.05. †Significantly greater than all others in the row, *P* < 0.05. ‡Significantly less than sample without inhibitor in same column, *P* < 0.05.

Table 4. Blood and bone marrow cell counts

Time	Not Injected				Injected			
	Blood		Bone marrow		Blood		Bone marrow	
	Air	HBO <sub>2</sub>	Air	HBO <sub>2</sub>	Air	HBO <sub>2</sub>	Air	HBO <sub>2</sub>
18 h								
Cells, ×10 <sup>6</sup> /ml	5.0±0.2	6.2±0.7	4.2±0.1	6.4±0.3	5.2±0.2	6.34±0.04	6.4±0.3	7.5±0.4
Leukocytes expressing CD34, %	0.30±0.02	0.63±0.01	13.4±0.2	28.1±3.3	0.2±0.05	0.81±0.08	28.1±3.3	38.7±3.1
5 days								
Cells, ×10 <sup>6</sup> /ml	5.2±0.3	7.4±0.1	4.8±0.1	18.9±0.8	5.6±0.1	7.6±0.48	12.2±3.5	47.6±0.4
Leukocytes expressing CD34, %	0.27±0.01	1.73±0.08	14.3±0.8	59.7±3.2	1.2±0.8	4.2±1.03	54.3±3.4	83.1±2.6
10 days								
Cells, ×10 <sup>6</sup> /ml	5.1±0.3	7.8±0.2	4.5±0.3	13.6±1.0	5.8±0.8	7.8±1.65	13.3±2.3	41.6±2.9
Leukocytes expressing CD34, %	0.29±0.02	0.97±0.05	14.9±0.4	65.6±3.7	1.6±0.04	5.8±2.5	68.7±4.0	91.3±2.9

Values are means ± SE, with  $n = 4$  for each time in the noninjected groups and  $n = 5$  for the injected groups. In the noninjected air-breathing, control groups, there are no significant differences among the blood or bone marrow cell counts and %CD34<sup>+</sup> cells. HBO<sub>2</sub>-exposed mice showed a significant increase in blood and bone marrow cells at 5 and 10 days vs. 18 h ( $P < 0.05$ , ANOVA). At each time point, the value for the HBO<sub>2</sub> animals is significantly different from that of the air-breathing group ( $P < 0.05$ , ANOVA). Among the groups of animals injected with Matrigel +/- lactide, air-breathing control and HBO<sub>2</sub>-exposed mice showed a significant increase in blood and bone marrow cells at 5 and 10 days vs. 18 h ( $P < 0.05$ , ANOVA). At each time point, the value for the HBO<sub>2</sub> animals is significantly different from that of the air-breathing group.

groups at each time point, are also shown. The GSH-to-GSSG ratio offers insight into the redox state of cells in each group. Cells from unsupplemented Matrigel of air-exposed control mice showed the highest ratio (most reduced state) at all time points. The ratio was significantly higher at 5 and 10 days than at 18 h for cells from unsupplemented Matrigel of air-exposed mice, and for all other groups the ratio was significantly higher at 10 days vs. 18 h, with variable degrees of differences at 5 days.

**SPCs in bone marrow and blood.** Table 4 shows leukocyte counts and fraction of cells positive for CD34 in blood and bone marrow. These data reflect the impact of Matrigel +/- lactide, as well as the effect of HBO<sub>2</sub>. If control mice are not injected with Matrigel + lactide and breathe only air, there is no significant change in blood or bone marrow cell counts or CD34<sup>+</sup> cell fraction over 10 days of observation. If mice are

injected with Matrigel + lactide, however, the growth factors released into the circulation by cells undergoing vasculogenesis in Matrigel have a systemic impact and increase circulating and bone marrow cell counts (42). HBO<sub>2</sub> by itself was found to have an influence separate from its effect on cells in Matrigel. In animals not injected with Matrigel but exposed daily for 90 min to 2.8 ATA O<sub>2</sub>, blood and bone marrow CD34<sup>+</sup> cell counts increased. Whereas the bone marrow CD34<sup>+</sup> cell count did not increase significantly between 5 and 10 days in any of the animal groups, we found a significant increase in blood CD34<sup>+</sup> cell count between 5 and 10 days in HBO<sub>2</sub> exposed mice injected with Matrigel +/- lactide.

**Roles for HIF transcription factors.** We have shown that HBO<sub>2</sub> enhances growth yield using cells removed from humans or mice exposed to HBO<sub>2</sub> and demonstrated that HIF-1 plays a central role in SPC recruitment to Matrigel (42, 60).

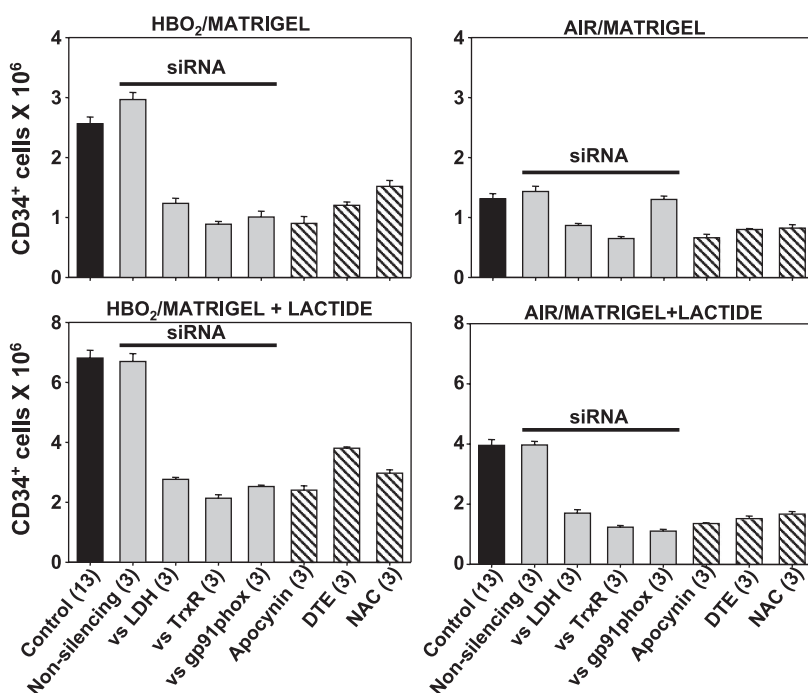


Fig. 3. CD34<sup>+</sup> cell numbers in Matrigel and effects with inclusion of small inhibitory RNA (siRNA), apocynin, or the anti-oxidants *N*-acetyl cysteine (NAC) or dithioerythritol (DTE). Bars identified as "vs LDH" show results when siRNA vs. lactate dehydrogenase (LDH) is included, "vs TrxR" bars show results when siRNA vs. thioredoxin reductase (TrxR) is included, and "vs gp91<sup>phox</sup>" bars show results when siRNA vs. the gp91<sup>phox</sup> NADPH subunit is included. Nos. in parentheses indicate no. of animals studied in each group. Cell nos. were significantly lower than the control value, except for samples containing nonsilencing (control) siRNA, and the air/Matrigel value for siRNA to gp91<sup>phox</sup>.

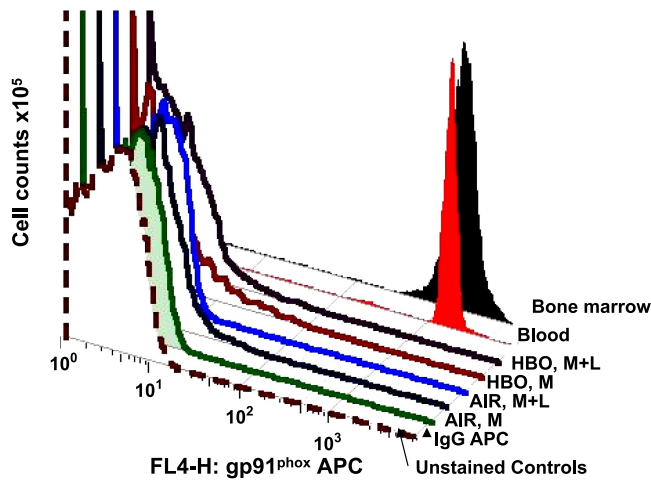
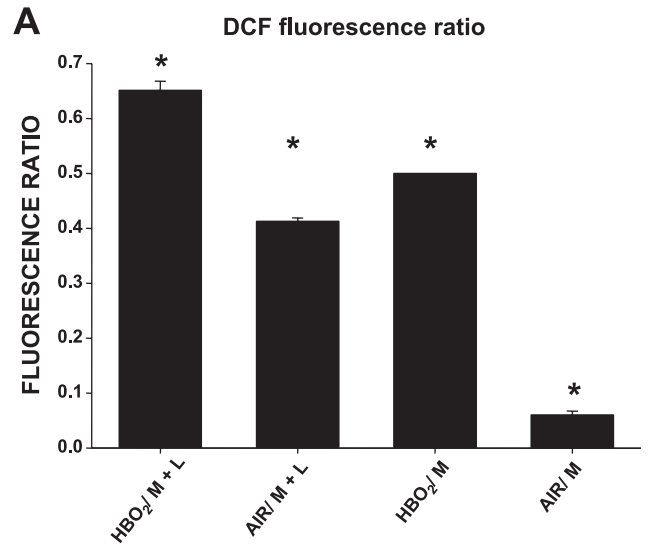


Fig. 4. siRNA reduces gp91<sup>phox</sup> protein in CD34<sup>+</sup> stem/progenitor cells (SPCs). These are representative data showing that CD34<sup>+</sup> cells isolated from Matrigel samples containing siRNA to gp91<sup>phox</sup> exhibit virtually none of this protein, in contrast to blood and bone marrow-derived CD34<sup>+</sup> cells from the same animals. These flow cytometry studies were performed by first selecting CD34<sup>+</sup> cells and then probing for intracellular expression of gp91<sup>phox</sup>. In cells from Matrigel containing siRNA to gp91<sup>phox</sup>, fluorescence was the same as that found in unstained cells and cells incubated with isotype control fluorochrome-conjugated antibody. Other labels shown in the figure are as follows: air M and air M+L, cell samples from unsupplemented Matrigel and Matrigel + lactide of an air-exposed control mouse, respectively; HBO<sub>2</sub> M and HBO<sub>2</sub> M+L, cell samples from unsupplemented Matrigel and Matrigel + lactide of an HBO<sub>2</sub>-exposed control mouse, respectively. APC, allophycocyanin.

Therefore, we examined the responses to HBO<sub>2</sub> in mice conditionally null for HIF-1 in myeloid cells (Table 5). The numbers of CD34<sup>+</sup> cells in the blood of air-breathing conditionally HIF-1 null mice were greater than in control mice, as we have previously reported (42), and HIF-1 null mice mobilized a significantly greater number of CD34<sup>+</sup> cells to the blood in response to HBO<sub>2</sub> exposure than did the control mice (Table 5). Despite the increase in blood cells, CD34<sup>+</sup> cell counts were significantly reduced in Matrigel harvested 18 h after implantation vs. counts in control mice. The reduction in CD34<sup>+</sup> cells in Matrigel +/- lactide from HIF-1 null mice was of similar magnitude, whether mice breathed just air or were exposed to HBO<sub>2</sub> (40–60%). Also, although SPCs recruitment to Matrigel 18 h after implantation was diminished in HIF-1 null mice, there were still significantly more CD34<sup>+</sup> cells in mice exposed to HBO<sub>2</sub> vs. responses in air-breathing control mice. We conclude from this that HIF-1 alone does not control HBO<sub>2</sub>-mediated responses.

Interestingly, non-SPC leukocyte influx, estimated by counting the number of CD45<sup>+</sup>/CD34<sup>-</sup> cells in Matrigel, exhibited the same pattern and magnitude of change in the genetically identical control mice (Table 5) as was found in normal, wild-type mice (Fig. 2). That is, in the HBO<sub>2</sub>-exposed mice, the number of CD45<sup>+</sup>/CD34<sup>-</sup> leukocytes in Matrigel was significantly lower than in the air-only exposed mice. However, the opposite pattern was observed in the HIF-1 null mice. The influx of CD45<sup>+</sup>/CD34<sup>-</sup> leukocytes into Matrigel was significantly higher in mice exposed to HBO<sub>2</sub> than those breathing just air. While the mechanism behind this difference is unknown, it may be related to differences in the total leukocyte counts in these mice. Air-breathing control mice had a cell count of  $5.4 \pm 0.2 \times 10^6/\text{ml}$  (mean  $\pm$  SE,  $n = 4$ ) with



**B** Catalase in SPCs and intracellular H<sub>2</sub>O<sub>2</sub> production

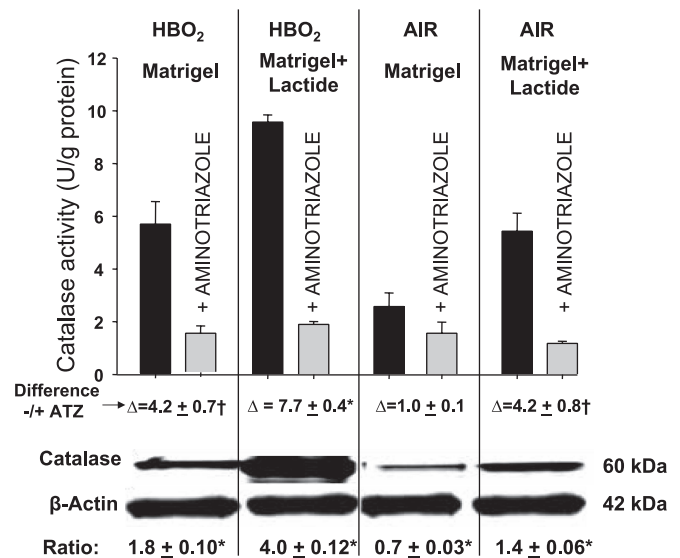


Fig. 5. A: 2',7'-dichlorofluorescein (DCF) fluorescence ratio. A H<sub>2</sub>DCF solution was placed on Matrigel samples mounted on a microscope stage, and DCF fluorescence was measured before and again after addition of 24 mM KCl to cause cell depolarization. Bar graphs show the means  $\pm$  SE of DCF fluorescence ratio (without vs. with KCl) from different Matrigel samples ( $n = 3$  different mice for each calculation). \*Significantly different from each other sample. B, top: cell lysate catalase activity, enzyme inhibition by 3-amino-1,2,4-triazole (ATZ), and cell catalase content. Cells were isolated from Matrigel +/- lactide after harvest from mice exposed to air or HBO<sub>2</sub>. Where indicated, ATZ was added to Matrigel before implantation to cause catalase inhibition, and the difference in catalase activity vs. samples without ATZ was used as an index of intracellular H<sub>2</sub>O<sub>2</sub> production. Values are means  $\pm$  SE ( $n = 3$  mice for all groups). The activity in ATZ-containing samples in the four groups was not statistically different; the catalase activity in samples without ATZ was significantly different except between HBO<sub>2</sub> unsupplemented Matrigel and air Matrigel + lactide. B, middle: differences ( $\Delta$ ) in catalase activity shown below the bar graph were calculated between samples -/+ ATZ using pairs of animals processed on the same day. \*The value for Matrigel + lactide in HBO<sub>2</sub>-exposed mice was significantly different from all other samples, whereas the two values with the  $\uparrow$  symbol were not different from each other, but were significantly different from the value for unsupplemented Matrigel in air-exposed control mice. B, bottom: below the ATZ data is a representative Western blot, and below that are data labeled "Ratio" that show the relative catalase content in cells as the mean density of catalase vs. actin on the same blot. These values are means  $\pm$  SE ( $n = 5$  for each group) \*Each value is significantly different from the others,  $P < 0.05$ .

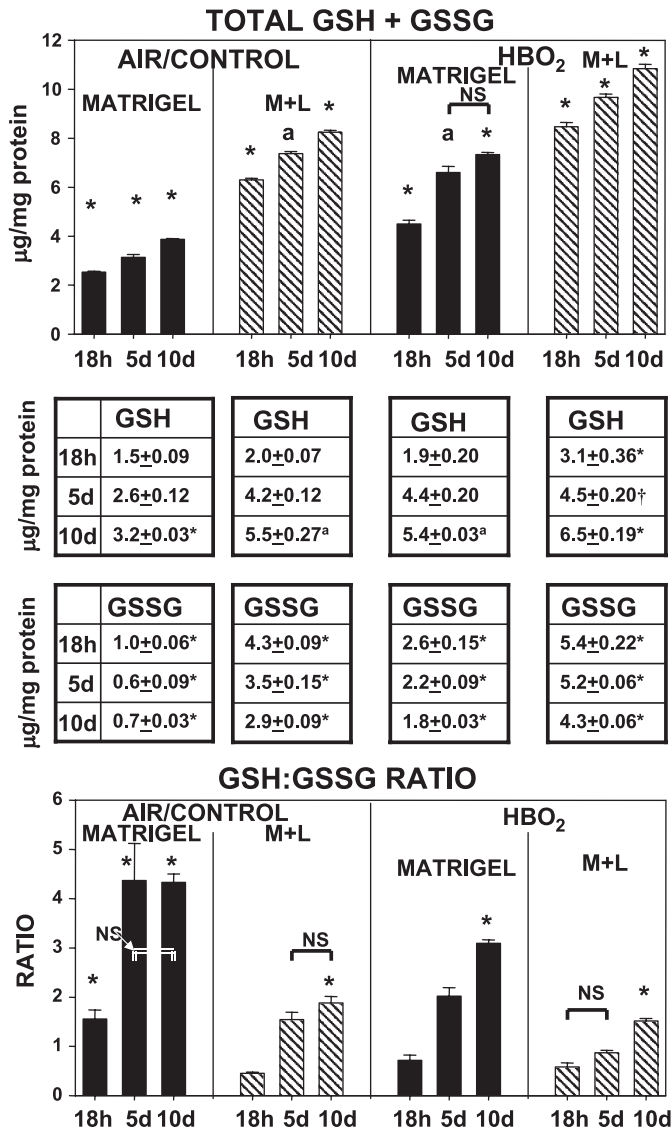


Fig. 6. Reduced (GSH) and oxidized glutathione (GSSG) levels in cells isolated from Matrigel samples. M+L, cells from Matrigel containing lactide. Values are mean  $\pm$  SE;  $n = 3$  for all groups. \* $P < 0.05$  vs. other samples from same time point (18 h, 5 or 10 days). <sup>a</sup>Significantly different from values at other time points, except that values with an "a" are not significantly different from each other. Note that, for bar graphs (total glutathione and GSH-to-GSSG ratio), the values at the three different time points within each group are significantly different, except for those marked NS (nonsignificant).

a nominal increase due to HBO<sub>2</sub> (to  $6.0 \pm 0.1 \times 10^6$ /ml). Air-breathing HIF-1 null mice had total leukocyte counts of  $5.9 \pm 0.5 \times 10^6$ /ml ( $n = 4$ , NS vs. control mice), but developed a leukocytosis of  $10.30 \pm 0.9 \times 10^6$  cells/ml ( $n = 4$ ,  $P < 0.05$ ) when exposed to HBO<sub>2</sub>.

Because there is functional redundancy among HIF factor isoforms, we examined the impact of incorporating siRNA to each of the three HIF factors in Matrigel. Use of siRNA to HIF-1 or -2 caused a significant inhibition of SPC recruitment vs. cell counts in wild-type controls and those containing nonsilencing siRNA in Matrigel samples (Table 6). Combining siRNA to HIF-1 and HIF-2 inhibited CD34<sup>+</sup> cell recruitment to a much greater extent than that caused by the individual

siRNAs. The presence of siRNA to HIF-3 led to a significant increase in SPC recruitment.

Table 7 shows the intracellular content of HIF transcription factors in CD34<sup>+</sup> cells and in CD45<sup>+</sup>/CD34<sup>-</sup> leukocyte isolated from Matrigel samples. In all samples, there was a significantly higher intracellular content of HIF factors in cells from mice exposed to HBO<sub>2</sub> vs. air-breathing controls. The suppressive effects of the various siRNA species on HIF synthesis can be seen in Matrigel samples containing these agents. There was a general pattern with marked suppression of transcription factors using siRNA for the specific HIF isoforms and, in some cases, statistically significant effects for other isoforms (e.g., when Matrigel included siRNA to HIF-1, there was a marked suppression of HIF-1 in CD34<sup>+</sup> and CD34<sup>-</sup>/CD45<sup>+</sup> cells and slightly reduced levels of HIF-3 in CD34<sup>+</sup> cells). Combining siRNA to HIF-1 and HIF-2 led to significant suppression of all HIF isoforms. These effects are described in the Table 7 legend.

*Trx system proteins and HIF expression.* Using flow cytometry, cells found in bone marrow and blood were harvested 18 h after Matrigel implantation and were partitioned between CD34<sup>+</sup> SPCs and leukocytes that express CD45 but not CD34, and intracellular expression of HIF-1, -2, and -3, TrxR, and Trx1 were evaluated (Fig. 7, A and B). Cells from mice exposed to HBO<sub>2</sub> exhibited significantly more of all factors. The magnitude of elevations in CD34<sup>+</sup> cells in bone marrow from control and HBO<sub>2</sub>-exposed mice were approximately twice as high as those found in blood, and CD45<sup>+</sup> cell protein levels were approximately one-eighth the levels found in CD34<sup>+</sup> cells. Expression of HIF-1, -2, and -3 proteins was significantly diminished in blood and bone marrow CD34<sup>+</sup> and CD45<sup>+</sup>/CD34<sup>-</sup> cells in mice conditionally null for HIF-1 in myeloid cells (Fig. 7C). Although not shown, the protein

Table 5. CD34<sup>+</sup> and CD34<sup>-</sup>/CD45<sup>+</sup> cells and recruitment to Matrigel 18 h after implantation into mice conditionally null for HIF-1 in myeloid cells vs. mice otherwise genetically identical

	Control	HIF-1 Null
Blood CD34 <sup>+</sup> , $\times 10^5$ /ml		
Air-only exposure	0.22±0.05	1.90±0.04
HBO <sub>2</sub>	0.45±0.04†	7.02±0.03†
CD34 <sup>+</sup> cells in Matrigel, $\times 10^6$		
Air-only exposure	1.37±0.04	0.89±0.03
HBO <sub>2</sub>	2.40±0.07†	1.33±0.09†
CD34 <sup>+</sup> cells in Matrigel + lactide, $\times 10^6$		
Air-only exposure	4.10±0.14	1.67±0.12
HBO <sub>2</sub>	6.33±0.19†	3.98±0.07†
CD 45 <sup>+</sup> /34 <sup>-</sup> cells in Matrigel, $\times 10^5$		
Air-only exposure	1.6±0.12	0.11±0.01
HBO <sub>2</sub>	0.09±0.006*	0.70±0.11†
CD 45 <sup>+</sup> /34 <sup>-</sup> cells in Matrigel + lactide, $\times 10^5$		
Air-only exposure	5.0±0.09	0.33±0.03
HBO <sub>2</sub>	2.4±0.21*	2.50±0.76†

Values are means  $\pm$  SE;  $n = 4$  animals. Values for CD34<sup>+</sup> and CD45<sup>+</sup>/CD34<sup>-</sup> cells are shown. Hypoxia-inducible factor (HIF)-1 null values, except the last line, are significantly different from control values. †HBO<sub>2</sub> value is significantly greater than corresponding air-only exposure value,  $P < 0.05$ . \*HBO<sub>2</sub> value is significantly less than corresponding air-only exposure value,  $P < 0.05$ . That is, in these mice, the CD45<sup>+</sup> cell influx into Matrigel was reduced by exposure to HBO<sub>2</sub>.

Table 6. *CD34<sup>+</sup> cell recruitment to Matrigel containing siRNA to HIF transcription factors*

	n	Air		HBO <sub>2</sub>	
		Matrigel	Matrigel + lactide	Matrigel	Matrigel + lactide
Control	5	1.33±0.10	4.21±0.18	2.64±0.13	7.01±0.31
+ siRNA (nonsilencing, control)	4	1.43±0.09	3.97±0.12	2.97±0.12	6.70±0.26
vs. HIF-1	3	0.93±0.07	1.50±0.04	1.73±0.09	3.94±0.04
vs. HIF-2	3	0.82±0.01	1.71±0.02	1.36±0.03	3.98±0.06
vs. HIF-3	3	2.25±0.19	6.93±0.09	3.87±0.15	8.71±0.32
vs. HIF-1 and HIF-2	3	0.26±0.03	0.56±0.03	0.45±0.03	1.13±0.15

Values are means ± SE of no. of cells; n, no. of animals in each group. Cell counts in Matrigel + lactide samples were significantly different from unsupplemented Matrigel, and all counts from mice exposed to HBO<sub>2</sub> were significantly greater than in air-only exposed, control mice. Inclusion of all agents except nonsilencing, control siRNA resulted in significantly different cell counts than control samples without inhibitor in same column. Notably, samples containing small inhibitory RNA (siRNA) to HIF-3 had more cells than control.

expression patterns for control mice otherwise genetically identical to the HIF-1 null mice were virtually identical to those of wild-type control mice.

**SPC cell cycle.** SPCs are not only recruited from bone marrow/blood to Matrigel, they appear to undergo proliferation, as shown in Table 3. To obtain greater insight into mitotic activity of CD34<sup>+</sup> cells in Matrigel, cell cycle progression was evaluated by determining the proportion of cells in the S and G<sub>2</sub>/M phases at 18 h after implantation. DNA content (propidium iodide uptake) was assessed by flow cytometry, and cell cycle was analyzed using computer software. The proportion of CD34<sup>+</sup> cells in S and G<sub>2</sub>/M phases in Matrigel or Matrigel + lactide samples from air-breathing and HBO<sub>2</sub>-exposed mice are shown in Fig. 8. As shown, agents that inhibit cell recruitment and protein synthesis also significantly inhibit cell cycle entry. Samples containing nonsilencing siRNA exhibited no significant changes compared with samples containing no extra agent, and samples containing siRNA to HIF-3 exhibited significantly greater cell cycle entry. Inhibitory agents impeded cell cycle entry, but they did not cause a higher proportion of cell to die based on propidium iodide staining. In cells isolated from unsupplemented Matrigel, there were 3.2 ± 0.21% (mean ± SE, n = 4) dead cells in samples from air-exposed control mice and 3.2 ± 0.10% (n = 4, nonsignificant) dead cells in samples from HBO<sub>2</sub> mice. No inhibitor caused significantly more cell death (data not shown). Similarly, no inhibitor caused a significant increase in cell death in samples isolated from Matrigel + lactide. Interestingly, however, there were slightly higher proportions of dead cells in samples from lactate-supplemented Matrigel vs. from unsupplemented Matrigel. There were 3.9 ± 0.26% (mean ± SE, n = 5, P < 0.05 vs. unsupplemented Matrigel from control mice) dead cells in Matrigel + lactide samples from air-exposed control mice and 4.6 ± 0.15% (n = 5, P < 0.05 vs. unsupplemented Matrigel from HBO<sub>2</sub>-exposed mice, but nonsignificant vs. Matrigel + lactide in air-exposed control mice) dead cells in samples from HBO<sub>2</sub> mice.

**Protein expression pattern in Matrigel-recruited cells.** SPCs exhibit a complex pattern of protein-protein interactions in which function of the Trx system and ERK1/2 MAPK influence HIF-1 synthesis and subsequent production of growth factors (42). With identification that the three HIF transcription factors influence SPC recruitment to Matrigel, we next evaluated the protein contents of cells in Matrigel harvested 18 h after implantation. Figure 9 shows relative changes normalized

to the values found in unsupplemented Matrigel from air-exposed, control mice. Similar values for air-exposed mice were presented in another publication (42), but those shown in the figure were studied concurrent with the HBO<sub>2</sub>-exposed mice. There was a consistent pattern for all proteins. Cells from HBO<sub>2</sub>-exposed mice demonstrated higher concentrations than cells from air-breathing, control mice, and cells from lactate-supplemented Matrigel had higher concentrations than cells from unsupplemented Matrigel. As shown, this pattern was consistent for HIF-1, HIF-2, and HIF-3, TrxR, Trx1, phosphorylated ERK, JNK and p38, VEGF, and SDF-1 (Fig. 9).

We hypothesized that HBO<sub>2</sub> poses an oxidative stress that stimulates SPC metabolism and cell recruitment to Matrigel. Consistent with this idea, CD34<sup>+</sup> cell recruitment and lactate effects on various proteins were inhibited in Matrigel that included apocynin, DTE, or NAC (Fig. 9). Trx1, as well as ROS, can stimulate MAPK phosphorylation and, in turn, ERK1/2 can stimulate Trx1 synthesis (3, 48). If U-0126, a specific ERK1/2 inhibitor, was included in Matrigel samples, a similar degree and pattern of inhibition is seen as with other agents, except there was no significant reduction in the fraction of phosphorylated p38 MAPK in unsupplemented Matrigel. U-0126 also inhibited CD34<sup>+</sup> cell influx compared with samples without inhibitors. Thus, in air-breathing, control mice, unsupplemented Matrigel plus U-0126 had 0.9 ± 0.08 × 10<sup>6</sup> CD34<sup>+</sup> cells (mean ± SE, n = 3, P < 0.05 vs. Matrigel without U-0126; compare with first line in Table 6), and in Matrigel + lactide there were 1.7 ± 0.10 × 10<sup>6</sup> (n = 3, P < 0.05). In HBO<sub>2</sub>-exposed mice, the number of CD34<sup>+</sup> cells in unsupplemented Matrigel containing U-0126 was 1.7 ± 0.12 × 10<sup>6</sup> (n = 3, P < 0.05), and in Matrigel + lactide the CD34<sup>+</sup> cell count was 3.4 ± 0.18 × 10<sup>6</sup> (n = 3, P < 0.05).

If Matrigel samples included siRNA to TrxR (but not nonsilencing, control siRNA), the increases seen in MAPK phosphorylation and the various proteins were abrogated, and numbers of CD34<sup>+</sup> cells in Matrigel were reduced (cell numbers are shown in Fig. 3). The same pattern of effects was also observed in samples containing siRNA to HIF-1 or HIF-2 and in the conditional HIF-1 null mice. HIF-3 appears to negatively modulate synthesis of SPC proteins surveyed in this investigation, as cells from Matrigel containing siRNA to HIF-3 exhibited significantly elevated protein levels.

Finally, consistent with the presence of an autocrine loop, antibodies to VEGF and SDF-1 also inhibited CD34<sup>+</sup> cell

Table 7. Intracellular content of HIF transcription factors in permeabilized CD34<sup>+</sup> and CD45<sup>+</sup>/CD34<sup>-</sup> cells from Matrigel assessed by flow cytometry

	CD 34 <sup>+</sup> Cells			CD 34 <sup>-</sup> /CD45 <sup>+</sup> Cells		
	HIF-1	HIF-2	HIF-3	HIF-1	HIF-2	HIF-3
Control						
Matrigel + lactide						
Air-exposed control mice	372.1±8.8	388.6±4.9	406.5±3.5	23.5±0.6	14.7±0.24	18.1±0.1
HBO <sub>2</sub> -exposed mice	708.7±33.4	717.1±8.1	726.8±25.5	40.0±0.75	35.4±0.95	39.0±0.09
Matrigel						
Air-exposed control mice	133.1±1.2	140.6±1.2	144.6±1.2	21.1±0.7	13.9±0.06	15.8±0.06
HBO <sub>2</sub> -exposed mice	197.1±1.4	241.9±7.01	294.2±4.6	28.4±0.61	26.2±0.38	30.0±0.46
siRNA control						
Matrigel + lactide						
Air-exposed control mice	355.2±6.4	400.6±5.4	396.1±4.6	24.1±0.4	15.4±0.25	19.4±0.4
HBO <sub>2</sub> -exposed mice	726.4±7.9	712.4±1.3	694.5±3.8	40.2±0.23	38.0±0.43	41.0±0.3
Matrigel						
Air-exposed control mice	131.3±0.8	141.6±1.8	132.3±0.8	22.2±0.9	14.4±0.17	18.9±0.2
HBO <sub>2</sub> -exposed mice	194.3±3.7	294.5±3.1	284.4±2.2	27.7±0.49	27.3±0.32	28.1±0.1
HIF-1 siRNA						
Matrigel + lactide						
Air-exposed control mice	27.7±0.70	394.9±5.7	298.7±6.8	2.20±0.17	15.7±0.21	19.1±0.4
HBO <sub>2</sub> -exposed mice	44.0±1.4	702.1±6.2	576.1±3.4	3.0±0.06	39.7±1.34	42.9±0.1
Matrigel						
Air-exposed control mice	11.2±0.2	141.4±1.6	106.6±2.9	1.23±0.03	15.2±0.23	16.2±0.3
HBO <sub>2</sub> -exposed mice	15.8±0.1	291.2±2.4	229.7±3.4	1.73±0.09	30.7±0.86	28.4±0.3
HIF-2 siRNA						
Matrigel + lactide						
Air-exposed control mice	465.1±5.5	27.8±0.73	24.5±0.6	21.6±0.3	2.23±0.14	22.1±0.5
HBO <sub>2</sub> -exposed mice	723±6.3	44.0±1.42	44.5±1.8	39.2±0.5	4.0±0.09	41.0±0.3
Matrigel						
Air-exposed control mice	136±3.4	11.2±0.23	13.0±0.19	14.0±0.4	1.8±0.06	19.7±0.1
HBO <sub>2</sub> -exposed mice	269.2±2.0	15.8±0.15	20.9±0.4	27.1±0.5	3.7±0.09	25.2±0.2
HIF-3 siRNA						
Matrigel + lactide						
Air-exposed control mice	480.1±11.3	402.6±4.9	22.3±1.4	25.7±0.4	23.5±0.5	2.4±0.09
HBO <sub>2</sub> -exposed mice	804.1±4.5	750.0±15.1	42.4±1.2	40.5±0.9	44.2±0.3	3.6±0.1
Matrigel						
Air-exposed control mice	142.1±1.7	139.2±3.5	12.2±0.2	22.8±0.5	21.7±0.1	1.2±0.09
HBO <sub>2</sub> -exposed mice	286.1±3.4	244.8±3.6	21.5±0.5	29.8±0.3	28.4±0.1	1.8±0.03
HIF-1 and -2 siRNA						
Matrigel + lactide						
Air-exposed control mice	15.9±0.7	17.0±0.6	36.8±1.1	1.5±0.1	1.9±0.1	2.6±0.1
HBO <sub>2</sub> -exposed mice	22.6±0.4	29.8±0.9	72.2±1.7	2.7±0.03	3.0±0.09	3.5±0.1
Matrigel						
Air-exposed control mice	8.9±0.2	11.5±0.5	15.1±0.1	0.9±0.05	1.1±0.1	1.5±0.1
HBO <sub>2</sub> -exposed mice	11.9±0.1	16.0±0.3	25.7±0.8	1.2±0.03	1.4±0.1	2.0±0.06
HIF-1 null						
Matrigel + lactide						
Air-exposed control mice	22.2±0.4	415.4±1.9	321.9±4.1	2.17±0.19	16.1±0.11	32.2±0.5
HBO <sub>2</sub> -exposed mice	40.2±0.6	707.0±1.8	673.6±22.7	2.87±0.18	37.2±0.50	49.5±0.4
Matrigel						
Air-exposed control mice	12.7±0.4	144.1±2.8	110.4±1.3	1.40±0.10	15.8±0.11	25.4±0.2
HBO <sub>2</sub> -exposed mice	18.2±0.2	320.1±9.4	245.9±8.6	1.73±0.03	27.6±0.78	36.1±0.09
HIF-1 null control						
Matrigel + lactide						
Air-exposed control mice	375.1±12.3	389.8±4.6	396.1±4.8	23.4±0.6	15.3±0.26	17.1±0.09
HBO <sub>2</sub> -exposed mice	745.3±29.0	694.5±3.76	749.8±16.4	39.9±0.8	42.7±0.89	35.1±0.1
Matrigel						
Air-exposed control mice	126.9±2.65	131.3±0.8	127.2±2.4	21.1±0.7	15.5±0.26	14.8±0.1
HBO <sub>2</sub> -exposed mice	197.9±4.0	184.4±2.2	215.9±1.9	28.4±0.6	28.5±0.61	27.8±0.4

Values are means ± SE of relative fluorescence units detected in cells in Matrigel removed from air-exposed, control mice and HBO<sub>2</sub>-exposed mice; *n* = 3 animals in each group. In all cases, values in HBO<sub>2</sub>-exposed mice were significantly different than those in air-exposed, control mice. Among CD34<sup>+</sup> cells, siRNA to HIF-1 significantly reduced levels of HIF-1 and had a small, but significant, effect on HIF-3. Mice conditionally null for HIF-1 had significantly different HIF-1 and HIF-2 levels vs. genetically identical controls, and slight but still significantly different HIF-3 levels in Matrigel + lactide samples and in the unsupplemented Matrigel samples from air-exposed, control mice. HIF-2 siRNA suppressed HIF-2 and HIF-3 and caused a small, but statistically significant, elevation in HIF-1 in Matrigel + lactide samples from HBO<sub>2</sub>-exposed and control mice, and in the unsupplemented Matrigel from HBO<sub>2</sub>-exposed mice. HIF-3 siRNA suppressed HIF-3 levels and significantly increased the levels of HIF-1 in all samples and HIF-2 in Matrigel + lactide samples. Combining siRNA with HIF-1 and HIF-2 caused suppression of all three HIF isoforms. In CD45<sup>+</sup>/CD34<sup>-</sup> leukocytes, siRNA to HIF-1 significantly reduced levels of HIF-1. Mice conditionally null for HIF-1 had decreased levels of HIF-1 and significantly increased levels of HIF-3. siRNA to HIF-2 suppressed HIF-2 and slightly reduced HIF-1 in unsupplemented Matrigel samples. siRNA to HIF-3 suppressed HIF-3 levels and increased the levels of HIF-2. Combining siRNA to HIF-1 and HIF-2 caused suppression of all three HIF isoforms.

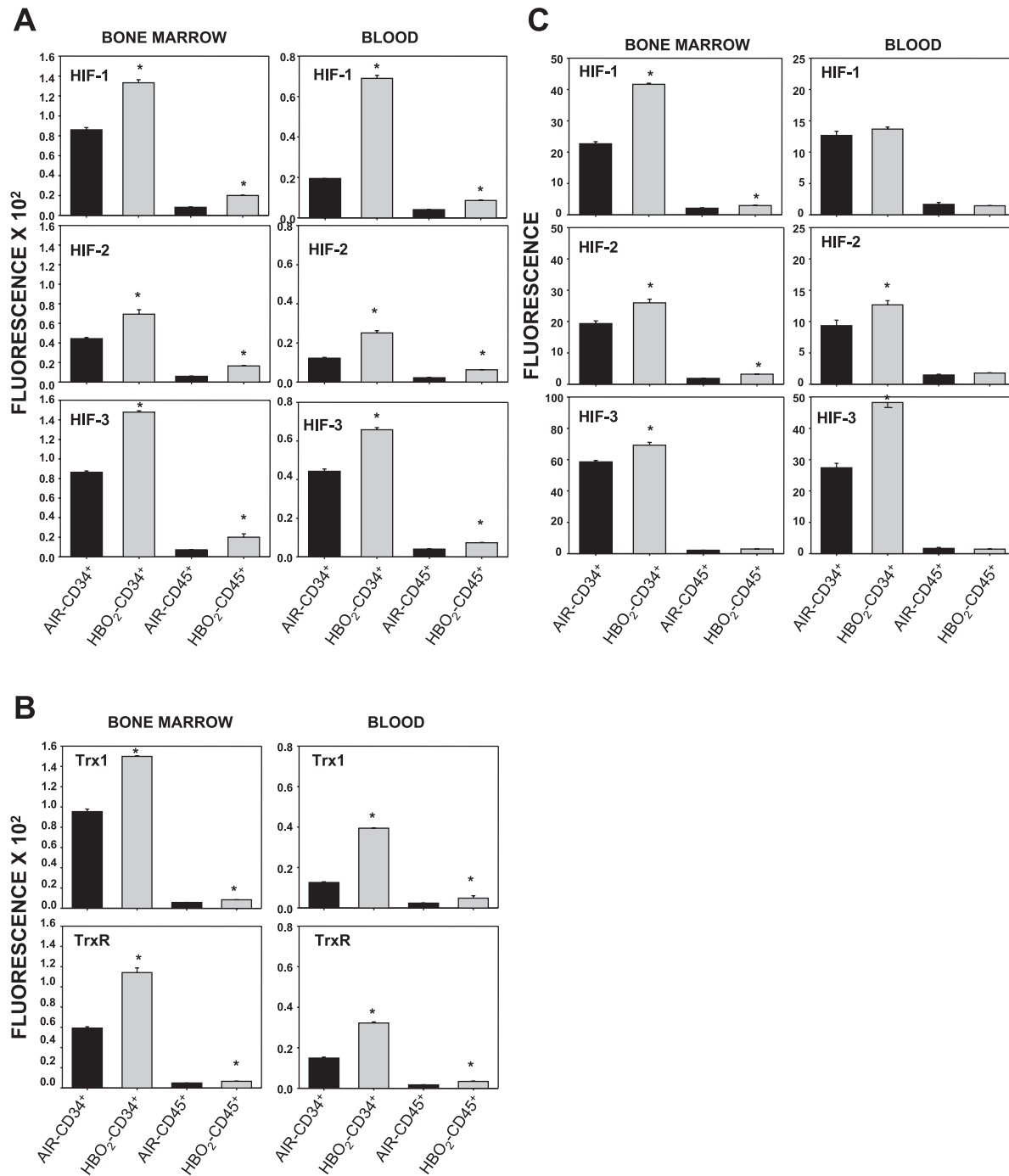


Fig. 7. Bone marrow and blood CD34<sup>+</sup> and CD45<sup>+</sup>/CD34<sup>-</sup> cell contents of hypoxia-inducible factor (HIF)-1, HIF-2, and HIF-3 (A), and thioredoxin 1 (Trx1) and TrxR (B) from flow cytometry analysis of permeabilized cells. C: HIF transcription factors in mice conditionally null for HIF-1 in myeloid cells. In all cases, protein levels in CD34<sup>+</sup> cells were significantly different from those in CD45<sup>+</sup>/CD34<sup>-</sup> cells. \*Significant difference between CD34<sup>+</sup> or CD45<sup>+</sup>/CD34<sup>-</sup> cells obtained from mice exposed to HBO<sub>2</sub> vs. control, air-breathing mice ( $n = 4$ ,  $P < 0.05$ ).

content of the various proteins, including VEGF and SDF-1. These antibodies also reduced SPCs recruitment. In air-breathing, control mice, Matrigel with anti-VEGF had  $0.55 \pm 0.01 \times 10^6$  CD34<sup>+</sup> cells (mean  $\pm$  SE,  $n = 4$ ,  $P < 0.05$  vs. unsupplemented Matrigel) and anti-SDF-1 had  $0.24 \pm 0.01 \times 10^6$  CD34<sup>+</sup> cells ( $n = 3$ ,  $P < 0.05$ ); in Matrigel + lactide with anti-VEGF, there were  $2.08 \pm 0.10 \times 10^6$  CD34<sup>+</sup> cells ( $n = 4$ ,  $P < 0.05$  vs. Matrigel + lactide without antibody), and with

anti-SDF-1 there were  $0.55 \pm 0.10 \times 10^6$  CD34<sup>+</sup> cells ( $n = 3$ ,  $P < 0.05$ ). In HBO<sub>2</sub>-exposed mice, the number of CD34<sup>+</sup> cells in Matrigel with anti-VEGF was  $1.01 \pm 0.04 \times 10^6$  CD34<sup>+</sup> cells ( $n = 4$ ,  $P < 0.05$  vs. Matrigel without antibody) with anti-SDF-1  $0.36 \pm 0.01 \times 10^6$  CD34<sup>+</sup> cells ( $n = 3$ ,  $P < 0.05$ ). In HBO<sub>2</sub>-exposed mice, the CD34<sup>+</sup> cell count in Matrigel + lactide with anti-VEGF was  $3.25 \pm 0.02 \times 10^6$  ( $n = 4$ ,  $P < 0.05$ ), and with anti-SDF-1 it was  $1.04 \pm 0.01 \times 10^6$  ( $n = 3$ ,  $P < 0.05$ ).

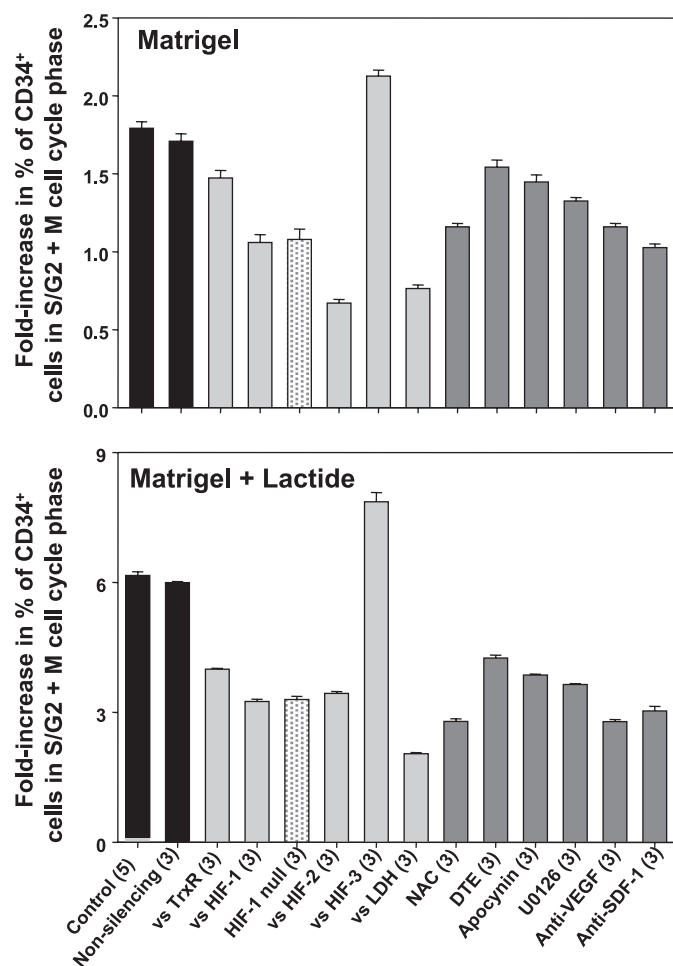


Fig. 8. Cell cycle data. Data reflect the increase in number of CD34<sup>+</sup> cells in S and G2/M phases from Matrigel or Matrigel + lactide 18 h after implantation in mice exposed to HBO<sub>2</sub>. These numbers are standardized to the percentage of CD34<sup>+</sup> cells entering the cell cycle (S, G2/M phases) in unsupplemented Matrigel 18 h after implantation in air-breathing, control mice, who had 3.83 ± 0.09% (*n* = 4) of CD34<sup>+</sup> cells in the S and G2/M phases. By comparison, CD34<sup>+</sup> cells from Matrigel + lactide harvested 18 h after implantation into air-breathing, control mice was 15.45 ± 0.3% (*n* = 4, *P* < 0.05). All values are significantly different from the control values (that indicate cells entering cell cycle in Matrigel or Matrigel + lactide with no additional agent), except the values where nonsilencing control siRNA was added. Note that the values for samples containing siRNA to HIF-3 are significantly greater than control samples.

## DISCUSSION

The Matrigel model allows for quantitative evaluations of in vivo SPC recruitment and growth responses, and inclusion of various inhibitory agents provides insight into regulatory mechanisms. An intricate network of channels within Matrigel was shown to connect to the mouse vasculature based on perfusion with fluorescent dextran or beads (Fig. 1). We conclude that this is a manifestation of vasculogenesis because channels were lined with CD34<sup>+</sup> cells, many also expressed the endothelial progenitor cell marker CD31, and many appeared to be undergoing proliferation based on expression of Ki67 (Fig. 1, Table 2).

HBO<sub>2</sub> and lactate each caused significantly greater channel formation based on Nile red bead fluorescence. The tight correlation between CD34<sup>+</sup> cell fluorescence and beads (Fig.

1B) suggests that most cells are incorporated into the vascular channels. At 18 h after implantation, over 90% of the cells present in Matrigel expressed CD34 as well as other surface markers for SPCs (Fig. 2, Tables 1 and 2). Matrigel + lactide exhibited a threefold increase in CD34<sup>+</sup> cells in air-breathing, control mice vs. unsupplemented Matrigel. In mice exposed to HBO<sub>2</sub>, there were twice as many CD34<sup>+</sup> cells in unsupplemented Matrigel vs. in the air-exposed control mice. The CD34<sup>+</sup> cell count was increased 5.5-fold in Matrigel + lactide for HBO<sub>2</sub>-exposed mice, indicating that HBO<sub>2</sub> and lactide had additive effects.

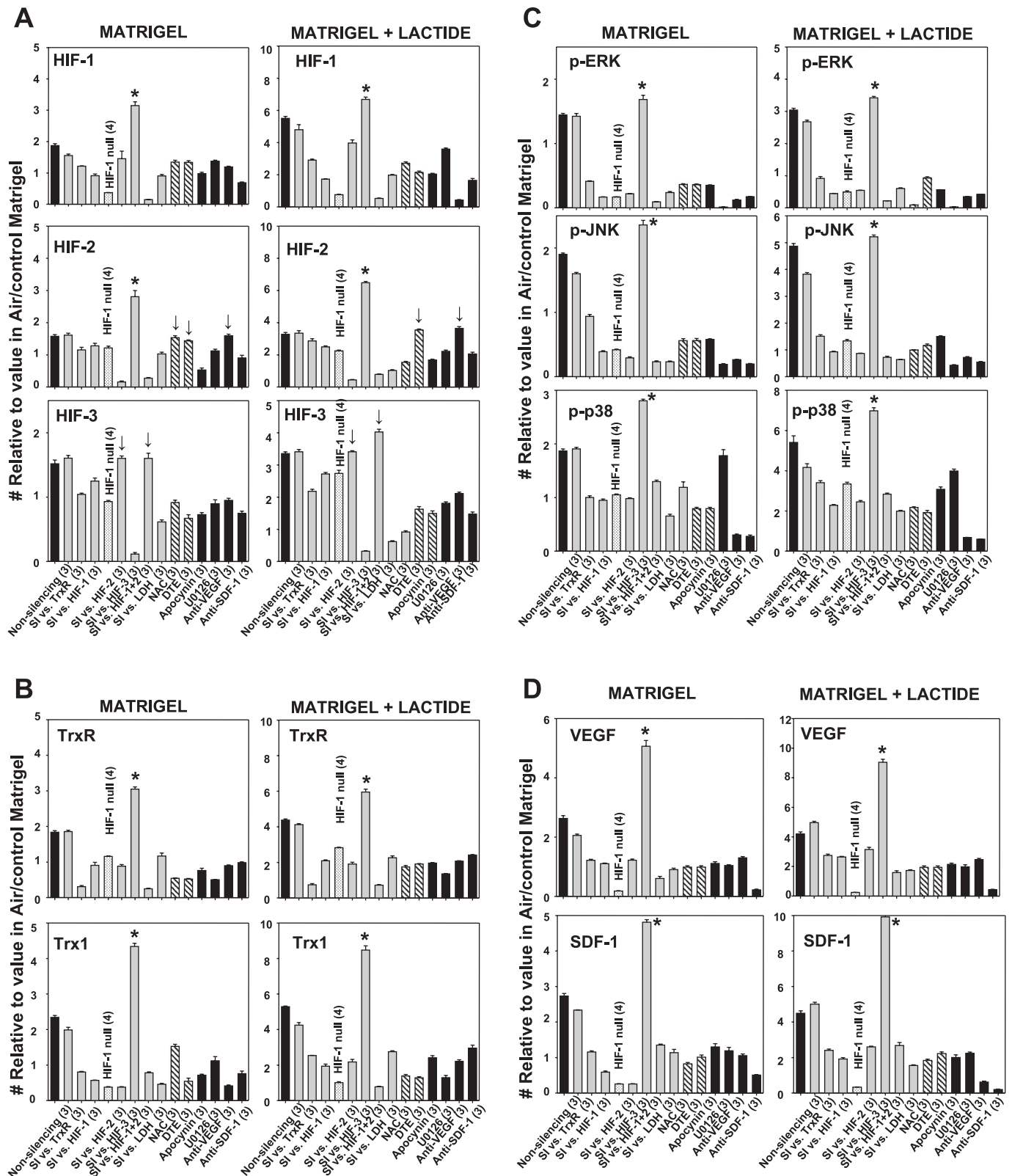
Studies with mitomycin C indicate that the differences in CD34<sup>+</sup> cell counts at 18 h postimplantation are due to recruitment of cells from the circulation vs. local proliferation (Table 1), but results in Table 3 demonstrate that exposure to HBO<sub>2</sub> has a functional impact as well. The ex vivo incubation of Matrigel shows that cell growth rate is increased and differentiation (based on surface marker expression) is modified due to prior HBO<sub>2</sub> exposure and also the presence of lactate. Whereas a very small fraction of CD34<sup>+</sup> cells in Matrigel expressed CD45 at 18 h postimplantation, the proportion increased significantly in Matrigel after 7-day incubation. Inhibition caused by inclusion of oxamate or antibodies to VEGF or SDF-1 indicates that ex vivo cell growth/differentiation involves LDH activity and growth factor production.

Our laboratory has reported that HBO<sub>2</sub> stimulates SPC mobilization by activating bone marrow nitric oxide synthase (15, 60). The CD34<sup>+</sup> blood cell counts (Table 4) are consistent with this observation. Lactate-supplemented Matrigel and HBO<sub>2</sub> also caused elevations in bone marrow CD34<sup>+</sup> cell counts. The elevations in CD34<sup>+</sup> bone marrow cells caused by lactate-supplemented Matrigel are thought to be related to growth factors liberated from the Matrigel that make their way back to bone marrow (42). This pathway is likely to occur in HBO<sub>2</sub>-exposed mice implanted with Matrigel, but additional mechanism(s) is operational, as bone marrow cell counts increased even in mice not implanted with Matrigel. CD34<sup>+</sup> cells exhibit significant elevations of Trx, TrxR, and the three HIF factors in animals exposed to HBO<sub>2</sub> (Fig. 7). This demonstrates the systemic effect of HBO<sub>2</sub> and indicates that SPCs in HBO<sub>2</sub>-exposed mice are primed to exhibit improved growth characteristics.

LDH can influence ROS production by providing NADH to Nox oxidases (18, 35), and this pathway appears to influence SPC responses based on the inhibitory effects of siRNA to LDH, gp91<sup>phox</sup>, apocynin, NAC, and DTE (Fig. 3). These agents exhibit an adverse effect on CD34<sup>+</sup> cell recruitment and differentiation in unsupplemented Matrigel, which we believe occurs because unsupplemented Matrigel contains ~3 mM lactate. These agents virtually negate the stimulatory effect of HBO<sub>2</sub> in unsupplemented Matrigel and significantly suppress the effect of HBO<sub>2</sub> in Matrigel + lactide. Results are consistent with the idea that HBO<sub>2</sub> stimulates SPC growth and differentiation by causing cellular oxidative stress. We directly demonstrated augmented ROS production by HBO<sub>2</sub> as elevated DCF fluorescence and also ATZ-mediated catalase inhibition in cells recruited to Matrigel (Fig. 5). An oxidative stress response was shown in these cells as increased expression of catalase and a modest shift in the GSH-to-GSSG ratio. The glutathione results were complex because all of the cell groups synthesized more glutathione per milligram protein over time.

At 18 h and at 5 days postimplantation, oxidative stress by lactate and by HBO<sub>2</sub> was demonstrated as a decrease in the GSH-to-GSSG ratio vs. the value in cells from unsupplemented Matrigel of air-exposed mice; although the differences

for samples containing lactide and/or exposed to HBO<sub>2</sub> were not significantly different from each other. Differences in GSH-to-GSSG ratios among these groups were present at 10 days, and the same general pattern persisted.

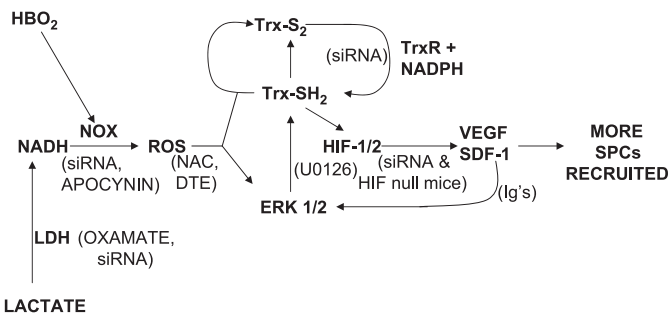


The Trx system responds to oxidative stress by reducing ROS and by promoting the expression and activity of HIF-1 (12, 26, 68). Trx1 can bind to a number of transcription factors and signaling molecules (40). We demonstrated a role for the Trx system in SPCs by the inhibitory actions of siRNA to TrxR (42). Findings in the present investigation indicate that, not only is there a complex interaction between Trx and HIF-1, but the Trx system also influences HIF-2 and HIF-3. This is a novel observation, and the complexity of the mechanism responsible for the enhancement is shown by finding that siRNA to TrxR diminished the content of Trx1, HIF-1, HIF-2, and HIF-3 in SPCs (Table 7 and Fig. 9).

When siRNA to TrxR, HIF-1, or HIF-2 was added to Matrigel, the number of CD34<sup>+</sup> cells present 18 h after implantation was reduced (Fig. 3, Table 6). Adding siRNA to both HIF-1 and -2 has a marked suppressive effect on SPC recruitment and protein synthesis (Table 6, Fig. 9). These results, along with findings in mice conditionally null for HIF-1 in myeloid cells (Table 5), indicate that HIF-1 and HIF-2 play positive trophic roles in the lactate- and HBO<sub>2</sub>-mediated effects. A suppressive role for at least one variant of HIF-3 has been reported (37, 41), but, to our knowledge, this study provides the first demonstration of its negative modulation of SPCs. That is, we show that siRNA to HIF-3 does indeed reduce HIF-3 content in SPCs (Table 7), and this reduction significantly stimulates SPC recruitment and protein synthesis in Matrigel (Table 6, Fig. 9).

Results in Table 3 and Figs. 8 and 9 demonstrate that blocking the action of VEGF or SDF-1 with antibodies will impair SPC growth and differentiation, consistent with previous trials (7, 22). Results in this investigation extend published reports by showing roles for HIF-2 and -3 in the autocrine feedback loop involving the Trx system and HIF-1- and HIF-dependent growth factors (42). All of the data in the present study are consistent with the idea that HBO<sub>2</sub> stimulates SPC growth and differentiation because it engages this physiological redox-sensitive autocrine activation loop (Fig. 10).

The inhibitory effects of apocynin and siRNA to the gp91<sup>phox</sup> subunit demonstrate that Nox plays a major role in augmented ROS production by hyperoxia, but other oxidase enzymes, mitochondria, and autooxidation of cellular components by molecular O<sub>2</sub> could also be involved. Because we find



LACTATE

Fig. 10. Diagram showing hypothesized sequence of effects triggered by HBO<sub>2</sub> and by lactate that stimulate SPC recruitment. Items in parentheses identify inhibitors used in this investigation to assess the roles of various agents in the pathway. Nox, NAD(P)H oxidases; ROS, reactive oxygen species; Trx-S<sub>2</sub>, oxidized thioredoxin; Trx-SH<sub>2</sub>, reduced thioredoxin; VEGF, vascular endothelial growth factor; Ig, antibodies to VEGF or SDF-1.

elevations of Trx1 and TrxR in SPCs from HBO<sub>2</sub>-exposed mice, we propose the pathway shown in Fig. 10 where physiological SPC activation occurs due to ROS from LDH activity, and HBO<sub>2</sub> feeds into this by augmenting production of ROS (42). It is important to point out, however, that these data do not rule out an impact from other regulatory systems. For example, modification of cell redox state due to mitochondrial activity impedes HIF prolyl hydroxylase activity, and a similar perturbation of redox state mediated by HBO<sub>2</sub> is feasible (47). There may also be involvement of activated phosphatidylinositol-3-kinase/Akt, NF-κB, or protein kinase C, because ROS play roles with activating these agents and their effects are inhibited by antioxidants like NAC (16, 24, 46). There could also be more direct effects of HBO<sub>2</sub>-generated ROS that impact HIF activation, such as oxidant-mediate ascorbate depletion or inhibition of phosphatases (8, 45).

Effects of the various inhibitors shown in Fig. 9A indicate that there are differences in the regulatory pathways for HIF transcription factors in SPCs. Reciprocal changes in cell content of the various HIF proteins were observed using siRNA to the HIF factors. That is, siRNA to HIF-3 resulted in elevations of HIF-1 and HIF-2 content. Elevations of HIF-3 were abrogated by siRNA to HIF-3 and also siRNA to HIF-1, but not when Matrigel contained siRNA to HIF-2. While siRNA to either

Fig. 9. Protein expression pattern in cells found in Matrigel. A: HIF-1, -2, and -3; B: TrxR and Trx1; C: p-ERK, p-JNK, and p-p38; D: VEGF and SDF-1. Cell lysates were subjected to Western blotting, as outlined in EXPERIMENTAL PROCEDURES. All values were normalized to the protein concentration found in cells isolated from unsupplemented Matrigel in air-exposed, control mice. The first solid bar in each graph is the value observed in Matrigel samples from HBO<sub>2</sub>-exposed mice without any inhibitors added. Agents were added to Matrigel or Matrigel + lactide as indicated on the abscissa. In all cases, wild-type mice were used, except for the bars indicated as HIF-1 null, where mice conditionally null for HIF-1 in myeloid cells were studied. Agents included in the Matrigel samples were nonsilencing, control siRNA, siRNA directed against TrxR, HIF-1, HIF-2, HIF-3, or LDH, NAC, DTE, apocynin, U-0126, anti-VEGF antibody, or anti-SDF antibody. The content of proteins in cells was expressed as the ratio of the band density on Western blots vs. β-actin on the same blot to control for differences in cell numbers. In all cases, non-silencing control siRNA had no significant effect on cell protein levels, and the protein content of cells isolated from Matrigel + Lactide was significantly greater than the value for cells isolated from Matrigel that did not contain Lactide. Unless otherwise noted in the figures, values for cells from Matrigel with inhibitors were significantly different from the values for cells isolated from Matrigel without the inhibitor. A: HIF-1 values (top) were elevated in Matrigel containing siRNA to HIF-3 (\*) and values using all other agents were lower than values for cells from Matrigel without inhibitors. HIF-2 values (middle) were higher in Matrigel containing siRNA to HIF-3. DTE and anti-VEGF had no significant effect on HIF-2 values in cells from Matrigel without or with Lactide (denoted by arrow). NAC had no significant effect on HIF-2 values in cells from Matrigel (shown by arrow), but it significantly reduced HIF-2 values in cells from Matrigel + Lactide. HIF-3 values (bottom) were not significantly reduced by siRNA to HIF-2 or when siRNA to HIF-1 and HIF-2 were combined (shown by arrow). B: TrxR and Trx-1 values were higher in Matrigel containing siRNA to HIF-3 and values using all other agents were significantly lower than values for cells from Matrigel without inhibitors. C: phosphorylated enzymes evaluated as a ratio compared to the total amount of the enzyme in cells. The fraction of phosphorylated enzyme was significantly greater than in cells from un-supplemented Matrigel. The fraction of phosphorylated enzyme in cells from samples with inhibitors was significantly reduced compared to the control cells except for those containing non-silencing, control siRNA and the phosphorylated p38 content in cells from un-supplemented Matrigel containing U0126. D: VEGF and SDF-1 values were significantly higher in Matrigel containing siRNA to HIF-3 and values using all other agents were significantly lower than values for cells from Matrigel without inhibitors.

HIF-1 or HIF-2 will reduce cell recruitment to Matrigel, intracellular content of HIF-2 in cells from HBO<sub>2</sub>-exposed mice is not significantly altered by DTE, NAC or anti-VEGF, in contrast to the effects of these agents on HIF-1 and also HIF-3. In cells from Matrigel + Lactide NAC, but not DTE, did pose an inhibitory effect on HIF-2. While there may be numerous explanations for these findings and more work is needed to discern responses to different agents, probably the simplest interpretation for most of the observations is that trophic effects in SPCs are more sensitive to alterations in HIF-1 than HIF-2.

There is ample precedence that oxidative stress has trophic effects of embryonic stem cells, endothelial progenitor cells, and skeletal and cardiac muscle precursor cells (34, 42, 43, 64). It is also clear that too much oxidative stress can have an adverse effect (19, 58). The clinical relevance of our findings is supported by use of an HBO<sub>2</sub> protocol that is in clinical use and prior demonstration that HBO<sub>2</sub> augments growth of SPCs from humans undergoing HBO<sub>2</sub> therapy for wound healing disorders (59, 60). No doubt there is a dose-response pattern to HBO<sub>2</sub> effects, but identification of protocols showing toxic effects on SPCs will require additional work.

It has been suggested that HBO<sub>2</sub> stimulates neovascularization by establishing a steep oxygen gradient at tissue margins, which has been thought to stimulate leukocyte recruitment and secondary growth factor release (23, 29, 30). Dim expression of CD45 is typically used to exclude leukocytes while enumerating SPCs (9, 27). We were surprised by how few leukocytes were present in all Matrigel samples harvested 18 h after implantation, and that there were significantly fewer leukocytes in samples from HBO<sub>2</sub>-exposed vs. air-exposed, control mice. Endothelial cells and macrophages increase VEGF synthesis when incubated in the presence of lactate (11, 33). The data from siRNA experiments indicate that augmented synthesis of growth factors by SPCs in lactate-supplemented Matrigel is due to HIF-1 and HIF-2 (Fig. 7). HBO<sub>2</sub> stimulates SPC metabolism following the same autocrine loop, thus suggesting ROS more so than an O<sub>2</sub> gradient per se drives neovascularization.

In summary, HBO<sub>2</sub> stimulates SPC growth and differentiation by engaging a physiological autocrine activation loop responsive to oxidative stress. Multiple lines of evidence demonstrate that HBO<sub>2</sub> influences CD34<sup>+</sup> cell recruitment and differentiation via a pathway involving Trx1, HIF-1, and HIF-2, with a suppressive action associated with HIF-3. Oxidative stress from HBO<sub>2</sub> acts in an additive manner with lactate to enhance vasculogenesis.

#### ACKNOWLEDGMENTS

This work was supported by grants from the Office of Naval Research and from the National Institutes of Health Grants DK080376 and GM081570.

#### REFERENCES

- Adams JD, Lauterburg BH, Mitchell JR. Plasma glutathione and glutathione disulfide in the rat: regulation and response to oxidative stress. *J Pharmacol Exp Ther* 227: 749–754, 1983.
- Ali M, Yasui F, Matsugo S, Konishi T. The lactate-dependent enhancement of hydroxyl radical generation by the Fenton reaction. *Free Radic Res* 32: 429–438, 2000.
- Andoh T, Chiueh C, Chock P. Cyclic GMP-dependent protein kinase regulates the expression of thioredoxin and thioredoxin peroxidase-1 during hormesis in response to oxidative stress-induced apoptosis. *J Biol Chem* 278: 885–890, 2003.
- Arai R, Masutani H, Yodoi J, Debbas V, Laurindo F, Stern A, Monteiro H. Nitric oxide induces thioredoxin-1 nuclear translocation: possible association with the p21Ras survival pathway. *Biochem Biophys Res Commun* 348: 1254–1260, 2006.
- Asahara T, Murohara T, Sullivan A, Silver M, van der Zee R, Li T, Witzenbichler B, Schatteman G, Isner JM. Isolation of putative progenitor endothelial cells for angiogenesis. *Science* 275: 964–967, 1997.
- Bennett M, Feldmeier J, Hampson N, Smees R, Milross C. Hyperbaric oxygen therapy for late radiation tissue injury. *Cochrane Database Syst Rev* Jul 20: CD005005, 2005.
- Ceradini DJ, Kulkarni AR, Callaghan MJ, Tepper OM, Bastidas N, Kleinman ME, Capla JM, Galiano RD, Levine JP, Gurtner GC. Progenitor cell trafficking is regulated by hypoxic gradients through HIF-1 induction of SDF-1. *Nat Med* 10: 858–864, 2004.
- Chandel N, McClintock D, Feliciano C, Wood T, Melendez J, Rodriguez A, Schumacker P. Reactive oxygen species generated at mitochondrial complex III stabilizes hypoxia-inducible factor-1 alpha during hypoxia. *J Biol Chem* 275: 25130–25138, 2000.
- Chin-Yee I, Keeney M, Anderson L, Nayar R, Sutherland D. Current status of CD34<sup>+</sup> cell analysis by flow cytometry: the ISHAGE guidelines. *Clin Immunol Newslett* 17: 21–29, 1997.
- Clarke R, Tenorio C, Hussey J, Toklu A, Cone D, Hinojosa J, Desai S, Parra L, Rodrigues S, Long R, Walker M. Hyperbaric oxygen treatment of chronic radiation proctitis: a randomized and controlled double blind crossover trial with long-term follow-up. *Int J Radiat Oncol Biol Phys* 72: 134–143, 2008.
- Constant JS, Feng JJ, Zabel DD, Yuan H, Suh DY, Scheuenstuhl H, Hunt TK, Hussain MZ. Lactate elicits vascular endothelial growth factor from macrophages: a possible alternative to hypoxia. *Wound Repair Regen* 8: 353–360, 2000.
- Ema M, Hirota K, Mimura J, Abe H, Yodoi J, Sogawa K, Poellinger L, Fujii-Kuriyama Y. Molecular mechanisms of transcription activation by HLF and HIF1 alpha in response to hypoxia: their stabilization and redox signal-induced interaction with CBP/p300. *EMBO J* 18: 1905–1914, 1999.
- Gallagher KA, Goldstein LJ, Buerk DG, Nedeau A, Xia M, Chen H, Thom SR, Liu ZJ, Velazquez OC. Diabetic impairments in NO-mediated endothelial progenitor-cell mobilization and homing are reversed by hyperoxia and SDF-1a. *J Clin Invest* 117: 1249–1259, 2007.
- Gladden L. Lactate metabolism: a new paradigm for the third millennium. *J Physiol* 558: 5–30, 2004.
- Goldstein LJ, Gallagher KA, Bauer SM, Bauer RJ, Baireddy V, Liu ZJ, Buerk DG, Thom SR, Velazquez OC. Endothelial progenitor cell release into circulation is triggered by hyperoxia-induced increases in bone marrow nitric oxide. *Stem Cells* 24: 2309–2318, 2006.
- Gorlach A, Diebold I, Schini-Kerth VB, Berchner-Pfannschmidt U, Roth U, Brandes RP, Kietzmann T, Busse R. Thrombin activates the hypoxia-inducible factor-1 signaling pathway in vascular smooth muscle cells: role of the p22(phox)-containing NADPH oxidase. *Circ Res* 89: 47–54, 2001.
- Grunewald M, Avraham I, Dor Y, Bachar-Lustig E, Itin A, Jung S, Chiment S, Landsman L, Abramovitch R, Keshet E. VEGF-induced adult neovascularization: recruitment, retention, and role of accessory cells. *Cell* 124: 175–189, 2006.
- Gupte S, Rupawalla T, Mohazzab H, Wolin M. Regulation of NO-elicited pulmonary artery relaxation and guanylate cyclase activation by HADH oxidase and SOD. *Am J Physiol Heart Circ Physiol* 276: H1535–H1542, 1999.
- Gurusamy N, Mukherjee S, Lekli I, Bearzi C, Bardelli S, Das D. Inhibition of Ref-1 stimulates the production of reactive oxygen species and induces differentiation in adult cardiac stem cells. *Antioxid Redox Signal*; doi:10.1089/ars.2008.
- Hailey D, Jacobs P, Perry D, Chuck A, Morrison A, Bondreau R. *Technology Report: Adjunctive Hyperbaric Oxygen Therapy for Diabetic Foot Ulcer: An Economic Analysis*. Ottawa, Ontario, Canada: Canadian Agency for Drugs and Technologies in Health, 2007, report no. 75.
- Hattori I, Yakagi Y, Nozaki K, Kondo N, Bai J, Nakamura H, Hashimoto N, Yodoi J. Hypoxia-ischemia induces thioredoxin expression and nitrotyrosine formation in new-born rat brain. *Redox Rep* 7: 256–259, 2002.
- Hattori K, Dias S, Heissig B, Hackett NR, Luyen D, Tateno M, Hicklin DJ, Zhu Z, Witte L, Crystal RG, Moore MA, Rafii S. Vascular endothelial growth factor and angiopoietin-1 stimulate postnatal hemato-

- poiesis by recruitment of vasculogenic and hematopoietic stem cells. *J Exp Med* 193: 1005–1014, 2001.
23. Hopf H, Uneo C, Aslam R R, Burnand K, Fife C, Grant L, Holloway A, Iafrafi M, Mani R, Misare B, Rosen N, Shapshak D, Slade B, West J, Barbul A. Guidelines for the treatment of arterial insufficiency ulcers. *Wound Repair Regen* 14: 693–710, 2006.
  24. Hwang K, Oh Y, Yoon H, Lee J, Kim H, Choe W, Kang I. Baicalein suppresses hypoxia-induced HIF-1 alpha protein accumulation and activation through inhibition of reactive oxygen species and PI 3-kinase/Akt pathway in BV2 murine microglial cells. *Neurosci Lett* 444: 264–269, 2008.
  25. Jin DK, Shido K, Kopp HG, Petit I, Shmelkov SV, Young LM, Hooper AT, Amano H, AVECILLA ST, Heissig B, Hattori K, Zhang F, Hicklin DJ, Wu Y, Zhu Z, Dunn A, Salari H, Werb Z, Hackett NR, Crystal RG, Lyden D, Rafii S. Cytokine-mediated deployment of SDF-1 induces revascularization through recruitment of CXCR4<sup>+</sup> hemangiocytes. *Nat Med* 12: 557–567, 2006.
  26. Kaga S, Zhan L, Matusmoto M, Maulik N. Resveratrol enhances neovascularization in the infarcted rat myocardium through the induction of thioredoxin-1, heme oxygenase-1 and vascular endothelial growth factor. *J Mol Cell Cardiol* 38: 813–822, 2005.
  27. Keeney M, Chin-Yee I, Weir K, Popma J, Nayar R, Sutherland D. Single platform flow cytometric absolute CD34<sup>+</sup> cell counts based on the ISHAGE guidelines. *Cytometry* 34: 61–70, 1998.
  28. Kina T, Ikuta K, Takayama E, Wada K, Majumdar A, Weissman I, Katsura Y. The monoclonal antibody TER-119 recognizes a molecule associated with glycophorin A and specifically marks the late stages of murine erythroid lineage. *Br J Haematol* 109: 280–287, 2000.
  29. Knighton DR, Hunt TK, Scheuenstuhl H, Halliday BJ. Oxygen tension regulates the expression of angiogenesis factor by macrophages. *Science* 221: 1283–1285, 1983.
  30. Knighton DR, Silver IA, Hunt TK. Regulation of wound-healing angiogenesis-effect of oxygen gradients and inspired oxygen concentration. *Surgery* 90: 262–270, 1981.
  31. Knowles H, Mole D, Ratcliffe P, Harris A. Normoxic stabilization of hypoxia-inducible factor-1a by modulation of the labile iron pool in differentiating U937 macrophages: effect of natural resistance-associated macrophage protein-1. *Cancer Res* 66: 2600–2607, 2006.
  32. Kranke P, Bennett M, Roedel-Wiedmann I, Debus S. Hyperbaric oxygen therapy for chronic wounds. *Cochrane Database Syst Rev*: CD004123, 2004.
  33. Kumar VBS, Viji RI, Kiran MS, Sudhakaran PR. Endothelial cell response to lactate: implication of PAR modification of VEGF. *J Cell Physiol* 211: 477–485, 2007.
  34. Lange S, Heger J, Euler G, Wartenberg M, Piper H, Sauer H. PDGF-BB stimulates vasculogenesis of embryonic stem cell-derived endothelial cells by calcium-mediated generation of reactive oxygen species. *Cardiovasc Res* 81: 159–168, 2009.
  35. Lee Y, Kang I, Bunker R, Kang Y. Enhanced survival effect of pyruvate correlates MAPK and NF(kappa)B activation in hydrogen peroxide-treated human endothelial cells. *J Appl Physiol* 96: 793–801, 2004.
  36. Lu H, Forbes R, Verma A. Hypoxia-inducible factor-1 activation by aerobic glycolysis implicates the Warburg effect in carcinogenesis. *J Biol Chem* 277: 23111–23115, 2002.
  37. Makino Y, Kanopka A, Wilson W, Tanaka H, Poellinger L. Inhibitory PAS domain protein (IPAS) is a hypoxia-inducible splicing variant of the hypoxia-inducible factor-3a locus. *J Biol Chem* 277: 32405–32408, 2002.
  38. Marx RE, Johnson RP, Kline SN. Prevention of osteoradionecrosis: a randomized prospective clinical trial of hyperbaric oxygen vs. penicillin. *J Am Dent Assoc* 111: 49–54, 1985.
  39. Massberg S, Konrad I, Schurzinger K, Lorenz M, Schneider S, Zohlhoefer D, Hoppe K, Schiemann M, Kennerknecht E, Sauer S, Schulz C, Kerstan S, Rudelius M, Seidl S, Sorge F, Langer H, Peluso M, Goyal P, Vestweber D, Emambokus NR, Busch DH, Frampton J, Gawaz M. Platelets secrete stromal cell-derived factor 1 alpha and recruit bone marrow-derived progenitor cells to arterial thrombi in vivo. *J Exp Med* 203: 1221–1233, 2006.
  40. Maulik N, Das D. Emerging potential of thioredoxin and thioredoxin interacting proteins in various disease conditions. *Biochim Biophys Acta* 1780: 1368–1382, 2008.
  41. Maynard M, Evans A, Shi W, Kim W, Liu FF, Ohh M. Dominant-negative HIF-3a4 suppresses VHL-null renal cell carcinoma progression. *Cell Cycle* 6: 2810–2816, 2007.
  42. Milovanova T, Bhopale VM, Sorokina EM, Moore JS, Hunt TK, Velazquez OC, Thom SR. Lactate stimulates vasculogenic stem cells via the thioredoxin system and engages an autocrine activation loop involving hypoxia inducible factor-1. *Mol Biol Cell* 28: 6248–6261, 2008.
  43. Mofarrahi M, Brandes R, Grolach A, Hanz J, Terada L, Quinn M, Mayaki D, BPetroff, Hussain S. Regulation of proliferation of skeletal muscle precursor cells by NADPH oxidase. *Antioxid Redox Signal* 10: 559–574, 2008.
  44. Nakamura H, Matsuda M, Furuke K, Kitaoka Y, Iwata S, Toda K, Inamoto T, Yamaoka Y, Ozawa K, Yodoi J. Adult T cell leukemia-derived factor/human thioredoxin protects endothelial F-2 cell injury caused by activated neutrophils or hydrogen peroxide. *Immunol Lett* 41: 75–80, 1994.
  45. Page E, Chan D, Giaccia A, Levine M, Richard D. Hypoxia-inducible factor-1 alpha stabilization in nonhypoxic conditions: role of oxidation and intracellular ascorbate depletion. *Mol Biol Cell* 19: 86–94, 2008.
  46. Page E, Robitaille G, Pouyssegur J, Richard D. Induction of hypoxia-inducible factor-1 alpha by transcriptional and translational mechanisms. *J Biol Chem* 277: 48403–48409, 2002.
  47. Pan Y, Mansfield K, Bertozzi C, Rudenko V, Chan D, Giaccia A, Simon M. Multiple factors affecting cellular redox status and energy metabolism modulate hypoxia-inducible factor prolyl hydroxylase activity in vivo and in vitro. *Mol Cell Biol* 27: 912–925, 2007.
  48. Pekkari K, Goodarzi M, Scheynius A, Holmgren A, Avila-Carino J. Truncated thioredoxin (Trx80) induces differentiation of human CD14<sup>+</sup> monocytes into a novel cell type (TAMs) via activation of MAP kinases p38, ERK, and JNK. *Blood* 105: 1598–1605, 2005.
  49. Piccoli C, D'Aprile A, Ripoli M, Scrima R, Boffoli D, Tabilio A, Capitanio N. The hypoxia-inducible factor is stabilized in circulating hematopoietic stem cells under normoxic conditions. *FEBS Lett* 581: 3111–3119, 2007.
  50. Rajantie I, Ilmonen M, Alminaita A, Ozerdem U, Alitalo K, Salven P. Adult bone marrow-derived cells recruited during angiogenesis comprise precursors for periendothelial vascular mural cells. *Blood* 104: 2084–2086, 2004.
  51. Rankin E, Garcia A. The role of hypoxia-inducible factors in tumorigenesis. *Cell Death Differ* 15: 678–685, 2008.
  52. Sachi Y, Hirota K, Masutani H, Toda K, Okamoto T, Takigawa M, Yodoi J. Induction of ADF/TRX by oxidative stress in keratinocytes and lymphoid cells. *Immunol Lett* 44: 189–193, 1995.
  53. Salceda S, Caro J. Hypoxia-inducible factor 1 alpha protein is rapidly degraded by the ubiquitin-proteasome system under normoxic conditions: its stabilization by hypoxia depends upon redox-induced changes. *J Biol Chem* 272: 22642–22647, 1997.
  54. Semenza G. Surviving ischemia: adaptive responses mediated by hypoxia-inducible factor 1. *J Clin Invest* 106: 809–812, 2000.
  55. Semenza GL. HIF-1 and mechanisms of hypoxia sensing. *Curr Opin Cell Biol* 13: 167–171, 2001.
  56. Sen C, Khanna S, Babior B, Hunt T, Ellison E, Roy S. Oxidant-induced vascular endothelial growth factor expression in human keratinocytes and cutaneous wound healing. *J Biol Chem* 277: 33284–33290, 2002.
  57. Sivan-Loukianova E, Awad OA, Stepanovic V, Bickenbach J, Schatteman GC. CD34<sup>+</sup> blood cells accelerate vascularization and healing of diabetic mouse skin wounds. *J Vasc Res* 40: 368–377, 2003.
  58. Sorrentino S, Bahlmann F, Besler C, Muller M, Schulz S, Kirchhoff N, Doerries C, Horvath T, Limbourg A, Limbourg F, Fliser D, Haller H, Drexler H, Landmesser U. Oxidant stress impairs in vivo reendothelialization capacity of endothelial progenitor cells from patients with type 2 diabetes mellitus. *Circulation* 116: 163–173, 2007.
  59. Thom S, Milovanova T. Hyperbaric oxygen therapy increases stem cell number and HIF-1 content in diabetics (Abstract). *Undersea Hyperb Med* 35: 280, 2008.
  60. Thom SR, Bhopale VM, Velazquez OC, Goldstein LJ, Thom LH, Buerk DG. Stem cell mobilization by hyperbaric oxygen. *Am J Physiol Heart Circ Physiol* 290: H1378–H1386, 2006.
  61. Thom SR, Xu YA, Ischiropoulos H. Vascular endothelial cells generate peroxynitrite in response to carbon monoxide exposure. *Chem Res Toxicol* 10: 1023–1031, 1997.
  62. To LB, Haylock DN, Simmons PJ, Juttner CA. The biology and clinical uses of blood stem cells. *Blood* 89: 2233–2258, 1997.
  63. Trabold O, Wagner S, Wicke C, Scheuenstuhl H, Hussain MZ, Rosen N, Seremetiev A, Becker HD, Hunt TK. Lactate and oxygen constitute a fundamental regulatory mechanism in wound healing. *Wound Repair Regen* 11: 504–509, 2003.
  64. Urao N, Inomata H, Razvi M, Kim H, Wary K, McKinney R, Fukai T, Mushio-Fukai. Role of Nox2-based NADPH oxidase in bone marrow

- and progenitor cell function involved in neovascularization induced by hindlimb ischemia. *Circ Res* 103: 212–220, 2008.
65. **Walenta S, Salameh A, Lyng H, Evensen J, Mitze M, Rofstad E, Mueller-Klieser W.** Correlation of high lactate level in head and neck tumors with incidence of metastasis. *Am J Pathol* 150: 409–415, 1997.
66. **Wang V, Davis D, Haque M, Huang L, Yarchoan R.** Differential gene-up regulation by hypoxia-inducible factor-1 alpha and hypoxia-inducible factor 2 alpha in HEK293T cells. *Cancer Res* 65: 3299–3306, 2005.
67. **Watson W, Heilman J, Hughes L, Spielberger J.** Thioredoxin reductase-1 knock down does not result in thioredoxin-1 oxidation. *Biochem Biophys Res Commun* 368: 832–836, 2008.
68. **Welsh S, Bellamy W, Briehl M, Powis G.** The redox protein thioredoxin-1 (Trx-1) increases hypoxia-inducible factor-1 alpha protein expression: Trx-1 overexpression results in increased vascular endothelial growth factor production and enhanced tumor angiogenesis. *Cancer Res* 62: 5089–5095, 2002.
69. **Yusa T, Beckman JS, Crapo JD, Freeman BA.** Hyperoxia increases H<sub>2</sub>O<sub>2</sub> production by brain in vivo. *J Appl Physiol* 63: 353–358, 1987.
70. **Zeigelhoeffer T, Fernandez B, Kostin S, Heil M, Voswinckel R, Helisch A, Schaper W.** Bone marrow-derived cells do not incorporate into the adult growing vasculature. *Circ Res* 94: 230–238, 2004.

